Global warming can be explained by depletion of stratospheric ozone caused by human activities and by volcanism

Peter L. Ward[1]

[1] U.S. Geological Survey retired, Teton Tectonics, Jackson, Wyoming, 83001-4875, USA

Correspondence to: P. L. Ward (peward@wyoming.com)

Abstract

Mean temperatures just above Earth‘s surface are thought to result from a delicate balance primarily between two sources of radiant energy: (1) solar energy, most of which warms Earth and its atmosphere directly during daytime, and (2) terrestrial infrared energy radiated outward from Earth 24 hours per day. Some spectral components of terrestrial energy are well observed to be absorbed by greenhouse gases in the atmosphere and are thought to warm the atmosphere, radiating back to Earth as much as 84% (Trenberth et al., 2009) of the infrared energy initially radiated by Earth. But only a small fraction of this terrestrial infrared energy is actually absorbed by greenhouse gases and less than half of that can be radiated back to Earth because radiation extends in all directions. Furthermore temperature in the troposphere decreases with altitude and a colder blackbody in the atmosphere cannot radiate back to Earth frequencies and amounts of energy high enough, according to Plancks law, to raise temperatures on Earth. You do not stand by a cold stove to get warm.

We explore here an alternate theory, that changes in mean temperatures on Earth result from changes in the mean amount of solar energy reaching Earth’s surface determined primarily by changes in the mean amount of ozone and of volcanic aerosols in the lower stratosphere. While greenhouse gases are well mixed throughout the atmosphere, ozone exists primarily in the lower stratosphere where concentrations vary regionally by 10% to as much as 50% on time scales of hours, seasons, decades, and longer. The catalytic processes of photodissociating and forming ozone again absorb solar ultraviolet energy, increasing the temperature of air very efficiently, over and over, heating the stratosphere. When the normal amount of ozone is depleted, less ultraviolet energy from Sun is absorbed in the stratosphere, the stratosphere cools, the tropopause rises, and more ultraviolet energy reaches Earth warming primarily the ocean and thereby raising mean surface air temperatures.

We document that the times and locations of major global warming observed over the past 60 years are contemporaneous with and co-located with the times and locations of greatest ozone depletion caused both by human activities (~3%) and by volcanic eruptions (~6% each), even small basaltic extrusive eruptions. Ozone depletion caused by humans and by two small, basaltic volcanoes in Iceland erupting in 2010 and 2011 totalled 14% in parts of central North America during the time and at the location of unusual warming and drought in 2012 and 2013. Detailed

observations of abrupt global warming in recent times and throughout geologic time are explained much more directly by depletion of stratospheric ozone than by changes in the concentrations of greenhouse gases. Based on our analysis, man's role in global warming may be far more manageable than currently thought.

1 Introduction

Earth's atmosphere is heated very efficiently by photodissociation where a molecule of gas absorbs sufficient oscillatory kinetic energy from a field of radiation to "shake apart" one or more of the chemical bonds holding the molecule together. Nearly all oscillatory kinetic energy originally within this bond plus nearly all oscillatory kinetic energy absorbed by this bond is converted directly into translational kinetic energy of the two pieces of the molecule flying apart and the temperature of a gas is, according to the ideal gas law, directly proportional to the average translational kinetic energy of all of its molecules. When the energy absorbed by any gas molecule is not energetic enough to cause dissociation, only a small fraction of this energy can be converted through collisions to translational kinetic energy and thus to an increase in temperature.

In order to develop an equation for the spectral radiance emitted by a black body as a function of temperature, Planck (1900) had to postulate that the energy in a field of radiation is equal to a constant times the frequency of the radiation. Energy contained within radiation can be thought of as the ability to cause photochemical change within a molecule and Planck's postulate fits clear observations that photosynthesis is caused by visible light having more energy than infrared radiation, that photodissociation is caused by ultraviolet radiation having more energy than visible light, and that X-rays have even greater energy than ultraviolet radiation. Nearly all photodissociation is caused by solar ultraviolet radiation.

The physical, chemical, and thermal structure of Earth's atmosphere is determined by how much high-frequency, high-energy solar ultraviolet radiation is available at each altitude. The highest energies are absorbed through photoionization of gases such as nitrogen and oxygen, forming the ionosphere at altitudes above 85 km. Lower energy radiation is absorbed in the mesosphere and stratosphere photodissociating oxygen. Still lower energy radiation photodissociates ozone initiating catalytic processes in the lower stratosphere that form and dissociate ozone over and over heating the lower stratosphere. When the amount of stratospheric ozone is depleted, it is this energy normally causing photodissociation and resulting warming of the lower stratosphere that is able to penetrate into the troposphere and down to Earth's surface.

The troposphere is heated primarily from below by a sun-warmed Earth while the stratosphere is heated primarily from above by solar radiation through photodissociation. The height of the tropopause decreases from the tropics to the poles and is observed to be very dynamic even on timescales of hours. When ozone in the lower stratosphere is depleted, stratospheric temperatures decrease, the tropopause rises, and more solar energy with wavelengths around 310 nm (nanometres) reaches the troposphere where it may be absorbed by some pollutants, but is primarily absorbed at Earth's surface. This is the same energy that causes sunburn and photodegradation of materials. Much of this energy is absorbed on land during the day and radiated back into the atmosphere at night. At sea, however, most

of this energy penetrates many metres and is only radiated back into the atmosphere when the whole surface layer of the ocean is warmed. Thus global warming appears to be driven more strongly by increases in ocean heat content that warms surface air temperatures rather than by increases in mean surface air temperatures.

The purpose of this paper is to examine evidence for the role of ozone depletion in climate change. In section 2 we will explore the physics of radiation and why Planck's law shows that radiation from cooler bodies cannot warm warmer bodies. In section 3 we will review how the energy content of solar radiation decreases as it descends thru the atmosphere, determining the chemical and physical structure of everything above the troposphere. The most dynamic part of the atmosphere is the optical thickness of the stratospheric ozone layer and we will see how this thickness determines how much high-energy solar radiation reaches Earth's surface. In section 4 we will note how the greatest warming is observed where and when ozone is most depleted. In section 5 we will review data showing that explosive volcanoes cool Earth while extrusive volcanoes warm Earth and in section 6 that all volcanic eruptions deplete ozone, even small, extrusive, basaltic eruptions. In section 7 we find that depletion of ozone by human activities and by the eruptions of Eyjafjallajökull (2010) and Grímsvötn (2011) in Iceland depleted ozone ~14% in the regions and at the times of major warming and drought throughout much of North America in 2012 and 2013. In section 8 we find that ozone depletion in the last 60 years is contemporaneous, within certain appropriate time delays, with 20th century warming. Section 9 provides conclusions and discusses what courses of action humans should take to reduce global warming. Appendix A describes several observations that do not seem to fit with greenhouse-gas theory. Appendix B describes apparent sudden emissions of ozone into the atmosphere weeks before volcanoes erupt. Appendix C looks more closely at the basic physics of electromagnetic radiation.

2 You do not stand by a cold stove to get warm

Temperature in matter is the macroscopic manifestation of the net kinetic energy of microscopic oscillations that pervade matter. Each degree of freedom of motion among and within atomic and molecular particles of matter oscillates about an equilibrium point between attractive and repulsive forces. The frequency of each oscillation is determined primarily by the physical properties of the degree of freedom such as the strength of the bond and the masses of the atoms or molecules involved. The spectral amount of oscillation at each frequency increases with temperature. When absolute temperature goes to zero, the amount of oscillation goes to zero. Raise the temperature (the kinetic energy of oscillation) high enough, the bonds lose their shear strength, forming a fluid. Continue to raise the temperature and all bonds holding the particles together come apart forming a gas where the bonds are reduced to collisions and the temperature therefore becomes proportional to the average kinetic energy of translation among all particles.

The kinetic energies of the various frequencies and amplitudes of oscillation are shared via conduction along all the interconnecting bonds or collisions so that after sufficient time, a region reaches thermal equilibrium with a broad distribution of frequencies and spectral amounts that vary with temperature similar to the shapes of the solid lines in Fig. 1. Motions of the electrons associated with atoms at the surface

of solid matter are thought to induce an electric field in air or in a vacuum that induces a magnetic field that induces an electric field, etc. forming electromagnetic radiation (EMR) spreading away from the surface. The spectral content of this radiation varies as a function of temperature as approximated by Planck's law for a black body, an idealized perfect absorber and emitter of radiation (Fig. 1). This spectral distribution of radiation most likely reflects the spectral distribution of oscillations at the surface of the radiating body that induced the radiation, much as the radiation from a radio transmitter reflects the frequencies of oscillation of charge within the antenna.

An alternate view is that the Universe is permeated by an energy field augmented locally by the conversion of mass to energy within stars, the burning of fossil fuels, and all other sources of energy. The physical properties of this field vary with the presence of matter rather than the field inducing or being induced by oscillations within matter (Appendix C).

In either case, we describe in matter at the macroscopic level the flow of this kinetic energy of microscopic oscillations as the flow of heat seeking thermal equilibrium. Energy flows from higher spectral amount to lower spectral amount (from higher temperature to lower temperature) and the rate of flow is proportional to the difference in spectral amounts (temperatures). The flow of energy via radiation can also be thought of as the flow of heat except we cannot see it, measure it, or perceive it until it interacts with matter. The physical mechanism by which radiation induces motion in dense matter is most likely similar to the physical mechanism by which motion in matter induces radiation. The flow of energy from radiation into matter, therefore, is most likely from higher spectral amount to lower spectral amount at the same frequency, much as a microwave oven warms water in food.

Planck (1900), in order to derive his equation for spectral radiance, the energy per second at each frequency emitted as radiation by a black body at a given temperature, had to postulate that the energy (E) contained within electromagnetic radiation in joules is equal to frequency (v, the Greek letter nu) times a constant of proportionality (h) so that this constant, known as Planck's constant, has units of joules per cycle per second. While in dimensional analysis it is customary to ignore cycles, this, according to Planck's postulate, ignores part of the fundamental units of energy. E=hv (dot-dash green line, Fig. 1) says that the energy contained within electromagnetic radiation is simply frequency and is not a function of anything else, including distance. This energy can be thought of as the ability to cause chemical change.

The net energy of electromagnetic radiation, on the other hand, is the energy at each frequency times the amount at each frequency (spectral amount) integrated across all frequencies. The spectral amount radiated is a function of the temperature of the source. Planck's law can be written as:

$$B(T) = E * A_1 * A_2 = (hv) * (1/\lambda^2) * (2/(e^{hv/kT}-1)) \quad (1)$$

where the spectral radiance (B) as a function of absolute temperature (T) of the surface of a black body is equal to the energy (E=hv) times a spectral amount (A_1) times another spectral amount (A_2). A_1 has some similarity to the Raleigh-Jeans law approximating the decay of spectral radiance with decreasing frequency (increasing wavelength λ); A_2 has some similarity to the Wien approximation governing the exponential decay of spectral radiance with increasing frequency (decreasing

wavelength). hv in A_2 is proportional to the mean energy of oscillation within a molecule per degree of freedom at a given frequency and kT is Boltzmann's constant (k) times absolute temperature (T), a product proportional to the mean kinetic energy of a gas molecule at a given temperature.

Since radiation spreads, the spectral amount of radiance received is equal to the spectral amount radiated ($A=A_1A_2$) divided by the square of the distance between the centre of the source and the surface of the receiver. Fig. 1 shows the spectral radiance emitted by Sun (red line) and the spectral radiance received at the top of Earth's atmosphere (Sun TOA, red dashed line). The energy (E) contained within the radiation, the frequencies, the colors of visible light, however, are well observed not to change over galactic distances unless there is motion between the source and the receiver. Thus for electromagnetic radiation, energy does not change with distance, but spectral amount (brightness) does.

This distinction between energy contained within radiation and the spectral amount of radiation is well illustrated by X-rays. It takes the high energy of X-rays (~12,400 eV, electron volts) to be able to travel through our bodies, but radiation with energy greater than ~3.9 eV begins to damage DNA, so the amount of X-rays used to examine our body must be at an extremely small dose (spectral amount) to prevent severe damage. Radiation treatment for cancer, on the other hand, focusses higher energy X-rays on cancerous cells in order to damage them.

The family of curves in Fig. 1, based on Planck's law, shows that both frequency and spectral amount at that frequency are functions of temperature. The observed frequency of the peak spectral amount can be calculated using Wien's displacement law as 5.88×10^{10} times the temperature T (dashed black line). To increase the temperature of matter, you must not only increase the spectral amount at every single frequency, but you must also increase the frequency of the peak spectral amount. Since spectral amount is a function of temperature, it takes radiation from a higher temperature body to increase the temperature of a lower temperature body. Even if the spectral amounts of radiation could somehow be added to the spectral amounts within warmer dense matter, which does not appear to be possible, there would still not be high-enough frequency energy to increase the frequency of the peak spectral amount. The microscopic oscillations within radiation appear to induce oscillations at the same frequency in matter so that heat flows from radiation into matter much as it flows from matter into radiation, from higher spectral amount to lower spectral amount. Higher temperature is associated with a higher rate of oscillation, which means higher frequency, which means higher kinetic energy of oscillation (E=hv), primarily in the ultraviolet (dot-dash green line, Fig. 1). Heat flows from higher energy to lower energy within matter and between radiation and matter. Radiation from a cooler body of matter cannot warm a warmer body of matter. You do not stand by a cold stove to get warm.

Greenhouse gas theory posits that greenhouse gases absorb infrared energy radiated by Earth, warming primarily the troposphere, reducing the ability of Earth to lose heat. This effect is shown by the fact that temperature in the troposphere decreases with altitude with a lapse rate averaging 5.5^oC/km for a wet atmosphere but 10^oC/km for a dry atmosphere. But efforts to balance Earth's energy budget (Trenberth et al., 2009; Trenberth and Fasullo, 2011) conclude that the surface radiates 396 W m^{-2} into the atmosphere and that the atmosphere radiates back to

Earth 333 W m^{-2}. Energy radiated by a colder layer of gas cannot warm a warmer Earth. Furthermore a layer of gas cannot be considered to be a black body because molecules of gas are not perfect absorbers of radiation; they are well observed to absorb energy from a radiation field only along narrow spectral lines (Rothman et al., 2009) within narrow spectral bands (Rohde, 2013). They only absorb a small portion of the energy contained in the surrounding electromagnetic field.

Furthermore, molecules of gas do not individually radiate energy in the infrared; this occurs only at much higher frequencies when electronic transitions are involved. The absorbed energy of oscillation is assumed to be converted to kinetic energy of translation via collisions according to the law of equipartition and then shared with all other gas molecules, raising the mean translational kinetic energy of the gas molecules, which is proportional to the temperature of a gas. The observed lapse rate shows that the amount of energy absorbed by greenhouse gases is insufficient to overcome the atmospheric rate of cooling. The smaller lapse rate for a wet atmosphere shows that greenhouse gases do slow the atmospheric rate of cooling, but the changes in energy are very small compared to the changes in ultraviolet energy described later in this paper because, by E=hv, energy contained in ultraviolet radiation at 310 nm (4.0 eV), energetic enough to photodissociate ozone, is 48 times the energy contained in infrared radiation at 1500 nm (0.083 eV), the centre of the broadest absorption peak for CO_2 (red circles, Fig. 1) and increase in temperature is proportional to increase in oscillatory kinetic energy. Furthermore, the peak spectral radiance of solar radiation at the top of the atmosphere (Sun TOA, dashed red line) is 69 times the peak terrestrial radiance just above Earth's surface (black line). The factor of 48, dependent on frequency, is contained within Planck's equation and is therefore contained within the factor of 69.

The total power (energy per second, watts) emitted by a black body is the integral of Planck's equation with respect to wavelength (frequency) and is equal to the Stefan-Boltzmann constant times temperature raised to the fourth power. The filament of an incandescent light bulb isolated in a partial vacuum has a temperature between 2000 and 3300K (purple line, Fig. 1) emitting a broad band of radiation that peaks in the infrared and feels hot. Only a small portion of this energy is within the visible spectrum producing useful light while most energy is usually wasted as heat. A typical fluorescent light bulb, on the other hand, causes the terbium, mercury, and europium coatings on the glass tube to fluoresce especially strongly at 542.4, 546.5 and 611.6 nm respectively emitting almost all the radiation within the visible spectral band accompanied by very little heat (white dashed lines over the visible spectrum in Fig. 1 in arbitrary units (Wikipedia, 2013b)). The integral with respect to wavelength (frequency) under these narrow spectral peaks is very small compared to the integral under Planck's curve. This is why fluorescent light bulbs and light emitting diodes are substantially more energy efficient than incandescent light bulbs, producing more useful light with less energy consumed. The energy absorbed by greenhouse gases is similarly along very narrow spectral lines, a small fraction of the broad spectrum of energy associated with heat (temperature).

The distinction between energy contained in radiation and amount of radiation is extremely important in studying climate change. First, the spectral distribution of energy contained in radiation leaving Sun, the ability to cause chemical change, is the same as the spectral distribution of radiation reaching the top of Earth's atmosphere; there is just a smaller amount of it, causing chemical change in fewer

molecules of gas. According to Planck's law, the amount of Sun's peak spectral radiance is 2.6 x 10^7 W sr^{-1} m^{-2} Hz^{-1} for a temperature of 5770K (Harder et al., 2009). The amount that reaches the top of Earth's atmosphere (TOA) is only 568 W sr^{-1} m^{-2} Hz^{-1}, which is Sun's peak spectral radiance times the square of Sun's radius divided by the square of the distance from the center of Sun to Earth (red solid and dashed lines, Fig. 1). When integrated across the appropriate solid angle and all frequencies, this value was observed recently to be between 1361 and 1362 W m^{-2} (ACRIM, 2013).

Second, the spectral distribution of solar energy headed toward polar regions is the same as the spectral distribution of solar radiation headed toward the tropics; there is just less amount of it falling on a square meter of Earth. But solar rays reaching polar regions are at a higher angle of incidence, traveling longer paths through the atmosphere, having a greater chance to interact with gas molecules such as by photodissociation of ozone. Not only does the ability to chemically deplete ozone increase during polar winters, but the ability to photodissociate ozone over mid to polar latitudes increases during winter, as does the possibility of more high-energy ultraviolet radiation reaching Earth when ozone is depleted.

3 Ozone depletion allows more solar ultraviolet energy to reach Earth

The dot-dashed green line in Fig. 2 shows the energy (E=hv) contained in electromagnetic radiation as a function of wavelength. The red line shows the spectral content of solar flux at the top of Earth's atmosphere (DeMore et al., 1997). Other lines show the spectral content of solar flux still remaining at altitudes of 50, 40, 30, 20 and 0 km in an average atmosphere (DeMore et al., 1997). While the observed spectral amount of Sun peaks at 451 nm and remains high throughout the visible spectrum (400 to 750 nm) (Gueymard, 2004), solar energy is highest and increasing at wavelengths <400 nm as shown by the dot-dashed green line.

The small amount of highest energy solar radiation in the extreme ultraviolet (λ<124 nm, E>10.0 eV) is typically absorbed at altitudes above 85 km causing photoionization primarily of N_2, O_2, and NO, forming the ionosphere. The large Lyman-alpha spectral peak (Fig. 2) radiated at 121.6 nm by hydrogen, which makes up 75% of Sun's mass, normally dissociates O_2, H_2O, and NO at altitudes above 70 km, but during solar maximums this peak can be 1.5 times larger than during solar minimums (Woods et al., 2000) and may not all be absorbed until well into the stratosphere. Note in Fig. 2 that essentially all of the solar energy for wavelengths <180 nm has been absorbed above 50 km by a variety of photochemical processes that do not need to be detailed here.

Photodissociation dominates at energy levels available in the mesosphere and stratosphere where densities, decreasing exponentially with increasing altitude, are still high enough to give practical meaning to the temperature of a gas. The net temperature of any gas depends not only on how many molecules exist but primarily on how much energy exists at frequencies high enough to cause ionization or dissociation. In fact the chemical structure of the atmosphere, the types and numbers of molecules, is primarily determined by the spectrum of solar energy available at a given altitude.

Photodissociation is a very efficient way to convert electromagnetic radiation into temperature of a gas because all the vibrational (oscillatory) kinetic energy originally contained in the bond plus all of the additional energy absorbed by the bond from the radiation field to sever the bond is converted into translational kinetic energy of the two separating atoms or molecules and, according to the kinetic theory of gases, the temperature of a gas is equal to the average translational kinetic energy of all of its atoms and molecules times a constant.

Modern chemical-transport climate models include more than 45 photodissociation reactions (Kinnison et al., 2007) occurring primarily at wavelengths less than 400 nm, shown for some important gases along the bottom axis of Fig. 2 (Turco, 1975; Hydutsky et al., 2008). In addition HO_2 is dissociated for λ<456 nm; HNO_3 for λ<598 nm; N_2O_5 for λ<750 nm (Turco, 1975).

Nitrogen (N_2), making up 78% of the volume of the atmosphere, persists primarily because it can only be destroyed (ionized) at energies >10 eV (λ<124 nm) (Wight et al., 2001). Oxygen (O_2), making up 21% of the atmosphere, is photodissociated into two ground-state oxygen atoms according to the following equation:

$$O_2 + hv(\lambda<242.4\ nm) \rightarrow O(^3P) + O(^3P) \quad (2)$$

which says that ultraviolet radiation with wavelengths less than 242.4 nm (frequency v>1240 terahertz) has sufficient energy (hv>5.11 eV) to sever the O_2 molecular bond forming two $O(^3P)$ ground state oxygen atoms (Finlayson-Pitts and Pitts, 1999). $O(^3P)$ then typically combines rapidly with O_2 to form ozone (O_3). O_2 has been dissociated in the laboratory for λ<248 nm (Slanger et al., 1988). Dissociation occurs over a much broader wavelength band due to details of the absorption process and energy added by various combinations of vibrational and rotational transitions. There is more than enough oxygen to absorb most of the solar wavelengths between 230 and 275 nm (Fig. 2) providing the primary heating of the stratosphere at altitudes of 15 to 50 km.

Quantitatively, the second most important photochemical reaction in the stratosphere is the photodissociation of ozone to form molecular oxygen and an $O(^1D)$ excited oxygen atom (Finlayson-Pitts and Pitts, 1999):

$$O_3 + hv(\lambda<310\ nm) \rightarrow O_2 + O(^1D) \quad (3)$$

when the wavelength (λ) is less than 310 nm (v>967 terahertz; hv>4eV).

There are many ways that the excited oxygen atom $O(^1D)$ can be deactivated to form an $O(^3P)$ ground state oxygen atom that reacts with O_2 to form ozone again.

Ozone makes up only ~0.002% of dry air, but unlike nearly all other important gases is not well mixed because its concentration depends on the relative amounts of energy available around 242.4 nm to produce ozone (dashed black line, Fig. 2) and around 310 nm to dissociate ozone (dotted black line). Ozone is typically formed, dissociated, and formed again catalytically so that net ozone can be thought of as a heating element powered by continued release of energy via photodissociation. Concentrations of ozone are greatest in the ozone layer between 15 and 35 km, but the thickness and concentrations of this layer vary seasonally and geographically.

The tropopause is the boundary between the troposphere heated primarily by a sun-warmed Earth from below and the stratosphere heated primarily via photodissociation caused by solar radiation. It also forms a boundary between low ozone mixing ratios in the troposphere and high ozone mixing ratios in the

stratosphere that contains more than 90% of total column ozone (Fioletov, 2008). The average height of the tropopause varies from 16.6 km near the equator where solar radiation is most intense to 9 km near the poles (Seidel and Randel, 2006). Annual mean heights increased ~160 m between 1980 and 2004 at the same time as northern mid-latitude total column ozone was depleted by ~4%, the lower stratosphere cooled ~2^{o}C, the upper troposphere warmed ~0.1^{o}C (Seidel and Randel, 2006), and mean surface temperatures in the northern hemisphere rose ~0.5^{o}C (HadCRUT3nh, 2013).

The photochemistry and physics behind global warming is shown more clearly in Fig. 3. The spectrum of radiation available from an overhead sun that normally reaches a given altitude is shown by actinic flux (AF), another way of looking at spectral radiance, as estimated by Madronich in Tables 3.7, 3.15, 3.16, 3.17 of Finlayson-Pitts and Pitts (1999). The increase in solar flux reaching the ground is confined to a very narrow bandwidth (red shaded area) (Madronich, 1993) between the rapidly increasing absorptivity of ozone below 350 nm (black line) (Rothman et al., 2009) and the very rapidly increasing availability of solar energy above 290 nm (red and purple lines). Between 1979 and 2008 at 50^{o}S, average solar ultraviolet flux under clear-sky conditions reaching Earth's surface was observed by satellite to increase 23% at 305 nm and 10% at 310 nm; at 50^{o}N, solar ultraviolet flux increased 9% at 305 nm and 4% at 310 nm (Herman, 2010).

Absorption by the ozone layer is essentially the difference in actinic flux at 40 and 15 km (dashed red and solid purple lines respectively). A 50% decrease in total column ozone will increase UV radiation at Earth's surface by ~2 W m^{-2} for overhead sun (red shaded area) and ~0.5 W m^{-2} for a solar zenith angle of 70^{o} (Madronich, 1993), likely, when integrated over the whole world, to cause most of observed global warming thought to be caused by an increase in radiation received at Earth's surface of ~0.9 W m^{-2} (Trenberth et al., 2009). The amount of heating will need to be calculated more precisely when atmospheric models have been improved to handle the issues regarding spectral radiance, photodissociation, and absorption discussed in this paper.

"From the time of Dobson's early measurements" in the 1920s, "it has been known that the total ozone amount undergoes large day-to-day fluctuations" (Reed, 1950; Fioletov, 2008) in the mid to high latitudes where the winter-time Brewer-Dobson circulation (Fig. 4a) brings stratospheric ozone formed mostly in the tropics down into the lower stratosphere and upper troposphere. Averages of these large changes are now mapped daily throughout the world as observed from satellites and ground stations (Figs. B1 and B3) (Environment Canada, 2013a). Animations of these daily ozone maps (Ward, 2013a, b) as well as measurements at each ground station (WOUDC, 2013) show that ozone amounts are continually changing even on timescales of minutes.

When total column ozone is depleted, less solar energy warms the stratosphere causing the tropopause to rise, allowing more UV radiation to be absorbed by Earth. When total column ozone increases, more solar energy is absorbed in the stratosphere, warming the stratosphere, lowering the tropopause, cooling Earth. Ozone accumulates over the Arctic in winter as shown in Fig. 4b (Fioletov, 2008), causing increased heating of the stratosphere and less heating of Earth resulting in minimum temperatures that are particularly cold during January in the Arctic and at

mid-latitudes when Arctic air masses move southward. Depletion of this polar ozone peak warms minimum winter temperatures and it is this warming of minimum winter temperatures that is most clearly observed as described below. The extremes of temperature are much larger during the winter when ozone accumulates and is depleted. For example, in Britain, the difference between record high and record low temperatures from 1870 thru 1999 was 47^{o}C during February-March and 38^{o}C during July (Webb and Meaden, 2012).

Early observations also showed "that there is a strong correlation between column ozone and meteorological conditions" (Reed, 1950; Fioletov, 2008) including atmospheric and surface temperatures and the resulting depth and location of surface pressure highs and lows. Ozone depletion allows more high-energy ultraviolet solar radiation into the lower troposphere where it either warms Earth directly or may warm the air through photodissociation of ground-level ozone, NO_2, or possibly absorption by SO_2 (Fig. 3). This warming can be across small regions and over timescales of hours to days, having a direct impact on weather systems.

On land, much of the energy absorbed during the day is radiated back into the atmosphere at night. At sea, however, ultraviolet radiation penetrates the ocean to depths >10 meters (Tedetti and Sempéré, 2006), making it more effective at heating the ocean than infrared radiation absorbed near the surface where much of the energy is lost back into the atmosphere at night. Similarly more ultraviolet energy is reflected back into the atmosphere on land than at sea. The effect of ultraviolet radiation on air temperatures could be small unless there is substantial lower-tropospheric pollution including O_3 and NO_2, while its effect on increasing ocean heat content could be substantial. The oceans account for 93% of the warming of the Earth system that has occurred since 1955 (Levitus et al., 2012).

In summary, molecules of gases in the atmosphere above the tropopause absorb primarily ultraviolet components of solar energy, causing photoionization, photodissociation and warming of the atmosphere above the tropopause. The atmosphere also reflects some solar energy back into space. When the atmosphere absorbs and/or reflects less solar ultraviolet energy than usual, more solar ultraviolet energy reaches Earth causing global warming. When the atmosphere absorbs and/or reflects more solar energy than usual, global cooling and ice ages occur. This filtering of solar radiation by the atmosphere is far more important for climate change than changes in solar radiance, which are generally <0.1% over 11-year cycles (Fröhlich and Lean, 1998).

4 The greatest warming occurred when and where ozone was most depleted

Depletion of ozone is thought to occur primarily in polar stratospheric clouds that form when temperatures drop below -78^{o}C within each polar vortex. The vortex centred over Antarctica forms in May and dissipates in October at latitudes greater than ~60^{o}S (Waugh and Polvani, 2010; Hassler et al., 2011). The Antarctic ozone hole typically reaches its maximum extent during September and its lowest values of ozone in late September to early October (NASA, 2013a). By 1989, ozone levels each October at Faraday/Vernadsky station near the Antarctic Peninsula (65.3^{o}S, 64.3^{o}W) had become depleted by ~45% compared to average levels from 1957 through 1970 (350 DU) (Hassler et al., 2011). Minimum yearly ozone levels throughout Antarctica have typically been depleted 45 to 55% relative to levels in

1979 (225 DU) when satellite measurements began (NASA, 2013a). During this time, the vortex has become “stronger, colder, and more persistent” (Waugh and Polvani, 2010).

The largest warming trend in the world observed between 1976 and 2000 was along the Antarctic Peninsula during the June-July-August time period continuing into the September-October-November as shown by Figure 2.10 of the report by the Intergovernmental Panel on Climate Change (IPCC) (Folland et al., 2001). Minimum monthly temperatures at Faraday/Vernadsky station increased 6.7^{o}C from 1951 to 2003 (Hughes et al., 2007), the greatest warming of this region in more than 1800 years (Vaughan et al., 2003; Mulvaney et al., 2012). These rapid increases in temperature “were strongly correlated” with decreases in total column ozone (Hughes et al., 2007). During summer months when ozone is not depleted, maximum monthly temperatures have changed very little since observations began. Between 1958 and 2010, annual mean temperatures increased 3^{o}C at Faraday/Vernadsky station and 2.4^{o}C at Byrd Station (80^{o}S, 199.5^{o}W) compared to 0.7^{o}C globally (Bromwich et al., 2013).

Decreased ozone allows more ultraviolet solar radiation to reach Earth’s surface where it is absorbed most efficiently by ice-free water, a band of which hundreds of kilometres wide exists off the ice-bound coast of Antarctica but still within the Antarctic ozone hole (Parkinson and Cavalieri, 2012). Summer surface temperatures of the Bellingshausen Sea rose 1^{o}C (Meredith and King, 2005), the Circumpolar Deep Water of the Antarctic Circumpolar Current warmed (Clarke et al., 2007), and formation of cold Antarctic Bottom Water decreased substantially (Purkey and Johnson, 2012). “Southern oceans have warmed at roughly twice the rate of global mean ocean” (Waugh et al., 2013).

Along the Antarctic Peninsula, winter sea ice decreased 10% per decade and shortened in seasonal duration (Clarke et al., 2007); 87% of the marine glaciers in this region retreated, many collapsing into the ocean following the loss of seven very large ice shelves (Clarke et al., 2007; Stammerjohn et al., 2008). Warming of interior Antarctica was slowed by the high mean albedo (~0.86) of Antarctic snow, nearly twice the albedo of Arctic snow (Wang and Zender, 2011), and by the decrease in solar flux approaching South Pole.

The Arctic is the region with the second greatest increase in surface temperatures (Folland et al., 2001; Trenberth et al., 2007). Ozone is depleted primarily during December, January and February within the Arctic polar vortex (Waugh and Polvani, 2010) but spreads south to mid-latitudes in spring enhanced by increasing NO_x-related “summer” depletion (Hansen and Chipperfield, 1999; Andersen and Knudsen, 2006). The asymmetric distribution of mountains, land, and ocean throughout the Arctic makes this vortex much more variable than the Antarctic vortex on daily to inter-annual time scales (Waugh and Polvani, 2010). The greatest amounts of total column ozone collect near and just outside the edge of the polar vortex in the polar night jet located throughout the stratosphere. Ozone concentrations change very dynamically as shown in the animations (Ward, 2013a, b) of daily ozone maps (Environment Canada, 2013a). Ozone depletion during winter/spring has been increasing in the Arctic since the 1950s, exceeding 80% at altitudes of 18 to 20 km in early 2011, comparable for the first time with the Antarctic ozone hole (Manney et al., 2011).

Temperatures north of 65°N increased at a rate of approximately twice the global average from 1965 to 2005 (Lemke et al., 2007). Annual mean land-surface temperatures north of 60°N increased 1.5°C between 1966 and 2003 (McBean et al., 2004; Jeffries and Richter-Menge, 2012) compared to 1.0°C for the northern hemisphere as a whole (CRUTEM4, 2013), unprecedented in the past 600 years (Tingley and Huybers, 2013). Satellite data from 1981 to 2005 for all areas north of 60°N show an average increase of 1.7°C with increases of 2.9°C over Greenland, 2.0°C over North America, 1.3°C over sea ice, and 0.3°C over Europe (Comiso, 2006). The average increase in monthly mean temperature from 1966 thru 2010 was >5°C north of 70°N, >4°C from 65° to 70°N, >1.5°C from 55° to 60°N and for the months of June through September was <2°C for all stations on land throughout the northern hemisphere (CRUTEM4, 2013).

The extent of Arctic sea ice, declining at >11% per decade since 1979 (Kwok and Untersteiner, 2011), reached a record low on September 16, 2012, nearly 50% lower than the average extent between 1979 and 2000 (NSIDC, 2012). The extent of terrestrial snow cover in June has decreased 17.8% per decade since 1979 (Derksen and Brown, 2012). Average snow-covered area in the northern hemisphere decreased ~7% primarily since 1982 (Lemke et al., 2007). Loss of ice in Greenland has been accelerating at a rate of 21.9 Gt/yr^2 (Rignot et al., 2011). The Canadian Arctic Archipelago has been losing ice at a rate of 61 Gt/yr (Gardner et al., 2011). Ice-cap melt rates on Ellesmere Island in the last 25 years have been the highest observed in 4200 years (Fisher et al., 2012).

The greatest rates of warming observed since the 1950s have been in Polar Regions during winter/spring when total column ozone has been most depleted.

5 Explosive volcanic eruptions cool Earth, but extrusive volcanic eruptions warm it

On June 15, 1991, Pinatubo volcano in the Philippines (15°N, 120°E) erupted ~5 km^3 of dacitic magma primarily within 9 hours, ejecting 17±2 Mt (megatons) of sulphur dioxide (SO_2) as much as at least 35 km into the stratosphere with peak mixing ratios observed via the SAGE II satellite of 300 ppbm decreasing to 160 ppbm within 180 days, and remaining above background for two years (Self et al., 1996). Within 21 days, SO_2 injected into the lower stratosphere had circled Earth and spread poleward to 30°N and 10°S. Within one year the SO_2 had spread throughout the globe. Approximately 13 Mt of erupted SO_2 (Self et al., 1996) ultimately was oxidized to form a nominally 75% sulphuric acid and 25% water aerosol primarily at altitudes between 20 and 25 km (McCormick and Veiga, 1992) with an e-folding time of aerosol formation in the tropics of ~35 days (Bluth et al., 1992) but as much as 13 months in the Arctic (Stone et al., 1993). The mid-visible (~500 nm) optical depth of the atmosphere increased to 0.3 within 2 months, peaked at 0.4 by late 1992, and averaged globally 0.1 to 0.15 for 2 years, thought to decrease solar radiation at Earth's surface by ~2.7 W/m^2 in August and 2.5 W/m^2 by late 1991 (Self et al., 1996). Surface temperatures decreased up to 0.6°C lower than normal in the northern hemisphere and averaged 0.4°C lower than normal over most of the globe thru 1993. However during the winters of 1991 and 1992, surface temperatures increased as much as 3°C above normal over North America, Europe, and Siberia (Robock, 2002). The lower stratosphere warmed as much as 3°C by mid-November, 1991, but cooled

to 0.35^{o}C below pre-eruptive levels by early 1993 (purple line, Fig. 6) (Labitzke and McCormick, 1992; Thompson and Solomon, 2009).

Most explosive volcanic eruptions of evolved magmas, such as andesite, dacite, and rhyolite, eject megatons of SO_2 within hours into the stratosphere, where, over weeks to months, the SO_2 gas is oxidized to form sulphuric acid vapour that coalesces onto condensation nuclei forming aerosols with particle sizes dominantly in the range of 300 to 500 nm (Deshler et al., 1993; Asano, 1993), large enough to reflect and disperse solar radiation causing global cooling of 0.3 to 0.6^{o}C for up to 3 years (Robock, 2000; Self, 2006). Modelling suggests that these 3 cooler years decrease temperatures in the upper two kilometres of oceans for decades (Gleckler et al., 2006a; Gleckler et al., 2006b) and that ocean cooling can accumulate (Gregory et al., 2006) incrementing the world into an ice age when large explosive eruptions occur every decade or so compared to only one in the past century (Ward, 2009). The number of layers of ash per thousand years from these types of volcanoes observed in marine cores off the west coast of Central America and throughout the Pacific (Kutterolf et al., 2012) are far more numerous during glacial periods than during interglacials.

Extrusive eruptions of primitive basaltic magma, on the other hand, extrude extensive lava flows for days, months, centuries, and even hundreds-of-thousands of years, emit 10 to 100 times more volatiles per cubic kilometre of magma (Palais and Sigurdsson, 1989; Freda et al., 2005; Self et al., 2008), do not eject most of these emissions high enough to reach the stratosphere, do not form extensive stratospheric aerosols, and cause net warming. The two largest in history were in South Iceland in the vicinity of the intersection of a developing east-west transform fault and the main spreading centre of the mid-Atlantic Ridge (Ward, 1971): Eldgjá, erupting 18 km^3 of basalt from 934 to 940 (Hjartarson, 2011), and Laki, erupting 15.1 km^3 from 8 June 1783 to 7 February 1784 (Thordarson and Self, 2003). Laki ejected ~24 Mt of SO_2 into the lower stratosphere but an additional ~96 Mt SO_2 into the troposphere where the jet stream carried much of it to the southeast toward Europe (Kington, 2009; Thordarson and Self, 2003). Severe acid damage to vegetation from Iceland to Eastern Europe, to Italy suggests concentrations of SO_2 could have been as high as 1000 ppb (Thordarson and Self, 2003), at least three orders of magnitude larger than background. A “dry fog” blanketed much of Europe primarily from mid-June through August. SO_2 is invisible but when absorbing ultraviolet radiation (Fig. 3), the electronic transitions cause fluorescence in the visible spectrum explaining the appearance of “dry fog”. There were ten major eruptive phases from June thru October. In July, surface temperatures in western Europe increased as much as 3.3^{o}C above the 30-year mean centred on 1783 (Thordarson and Self, 2003) and temperatures in Central England were the highest recorded from the first measurements in 1659 (Manley, 1974) until 1983 (Parker et al., 1992). SO_2 injected into the stratosphere would not have had adequate time to form aerosols during the many eruptive phases in July.

The Laki eruption deposited ~115 ppb sulphate in snow at Summit Greenland, 1500 km to the west-northwest (Zielinski et al., 1996). The layers of ice in the GISP2 borehole that contain the largest concentrations of volcanic sulphate per century (black line, Fig. 5) also contain $\delta^{18}O$ evidence (White et al., 1997) for the most rapid global warming (red line) during the Bolling warming, decreasing during the cooler Younger Dryas, and increasing again during the Preboreal warming. Volcanic

sulphate is total sulphate measured minus the small contributions from sea salt and dust determined by sodium and calcium content (Mayewski et al., 1997). Depletion of H_2O_2 associated with volcanic sulphate deposits in snow suggests that the SO_2 reached Greenland as a gas and was oxidized to sulphate during precipitation (Laj et al., 1990).

The temporal association of SO_2 emissions with warming at least in the Greenland region over the past 25,000 years shown in Fig. 5 is unambiguous. There is little error in relative timing between sulphate and the $\delta^{18}O$ proxy for temperature because both are measured in the same layers of ice. The ratio of signal to noise is very high. Peak sulphate per century during peak warming (2028 ppb) is 218 times greater than average sulphate per century (9.3 ppb) during the last glacial maximum (21 to 25 ka, thousand years before present) and 441 times greater than average sulphate (4.6 ppb) between 5 and 1 ka. More than 63% of the 7000 ice layers measured contain zero volcanic sulphate. In 2009, I tried to explain how the warming might be caused by SO_2 (Ward, 2009, 2010) but ultimately realized that sulphate and its precursor (SO_2) simply indicate the rate of volcanism per century and the likely amount of associated ozone depletion discussed in the next section.

Basaltic volcanism under ice forms long, flat-topped, steep-sided table mountains or tuyas found throughout Iceland. “12 of the 13 dated table mountains experienced their final eruptive phase during the last deglaciation” (Licciardi et al., 2007). Melting of ice might have increased magma production by decreasing the vertical loading on the top of the magma sources (Huybers and Langmuir, 2009). The relatively continuous high rate of most-likely basaltic volcanism shown in Fig. 5 from 11.7 to 9.8 ka, possibly assisted by increases in solar radiation due to Milanković cycles, was apparently sufficient to warm the ocean out of the last ice age.

Volcanism was similarly highest, primarily in Iceland, during the other 13 Dansgaard-Oeschger sudden warmings between 46 and 11.6 ka (Rahmstorf, 2003; Severinghaus, 1999) when regional surface temperatures rose to inter-glacial levels within a decade or two and then decreased back to ice-age temperatures over decades to centuries most likely as volcanism waned before the deep ocean could be warmed (Ward, 2009).

The Paleocene-Eocene Thermal Maximum was a brief period of extreme global warming beginning around 56.1 Ma (million years before present) as subaerial extrusion of basalts related to the opening of the Greenland-Norwegian Sea suddenly increased to rates greater than 3000 km^3 per kilometre of rift per million years (Storey et al., 2007) although basalt extrusion may have lasted only 220,000 years (Röhl et al., 2000). Global surface temperatures rose 5 to 9^oC within a few thousand years (Zeebe et al., 2009). Sea surface temperatures near the North Pole increased to 23^oC (Sluijs et al., 2006). Southwest Pacific sea surface temperatures rose rapidly to 34^oC, cooling back to 21^oC over seven million years (Bijl et al., 2009).

The Laki eruption in 1783 extruded 12.3 km^3 of lava flowing over an area of 565 km^2. Every 6 to 52 million years, 22 on average, there have been massive eruptions of 0.2 to 8 million km^3 of basalt in what have become known as Large Igneous Provinces (LIP), typically contemporaneous with major mass extinctions (Courtillot and Renne, 2003; Wignall, 2005; Ward, 2009).

At approximately 250 Ma, for example, at least 3 million km^3 of basalt was extruded in Siberia over an area of at least 5 million km^2 (equivalent to 62% of the contiguous

48 United States) possibly in less than 670,000 years (Reichow et al., 2009). Low-latitude surface seawater temperatures rose 8^{o}C (Joachimski et al., 2012), nearly 3 times the rise in tropical Pacific sea surface temperatures at the end of that last glaciation (Lea, 2000). “Lethally hot temperatures exerted a direct control on extinction and recovery” (Sun et al., 2012). There was massive depletion of ozone (Beerling, 2007). “Global warming and ozone depletion were the two main drivers for the end-Permian environmental crisis” (Svensen et al., 2009). “Prolonged exposure to enhanced UV radiation could account satisfactorily for a worldwide increase in land plant mutation” at this time (Visscher et al., 2004).

The most recent LIP was the Columbia River Basalts in Oregon and Washington States at approximately 16 Ma with an estimated volume of 174,300 km^3 (McBirney, 2007). A recurrence of even the smallest of these LIPs would be a major problem for mankind.

The differences between explosive and extrusive volcanism are summarized in Table 1. Basalt is the primitive magma rising from the mantle into the crust. When the crust is thin, as in ocean plateaus and ocean basins, hot basalt has enough buoyancy to rise to form sills and small magma chambers at a few kilometres depth and then to extrude out onto the surface with the minor dissolved gas content forming lava fountains and curtains of fire. Explosions are typically too small to eject substantial volcanic ash and gases into the stratosphere. Extrusions are typically very voluminous, accumulating over weeks to millennia. When the crust is thick, basalt can only rise to depths of 5 to 15 km where its heat content melts crustal materials, forming more evolved silicic magmas. Over hundreds to hundreds-of-thousands of years, the density of the magma decreases and the gas content increases until some magma can rise to the surface causing a large explosive eruption. Sometimes so much magma is ejected in a giant eruption that the overlying crust drops down into the magma chamber forming a caldera. Explosive eruptions tend to last only hours to days but an individual volcano may erupt again over intervals of centuries to hundreds-of-thousands of years.

Approximately 80% of all volcanism on Earth occurs along mid-ocean ridges, most of which lie more than 2 km below sea-level. These volcanoes do not have much direct effect on climate, but they do heat the ocean. Kump et al. (2005) argue that massive release of hydrogen sulphide from submarine volcanoes during anoxic intervals of Earth history would cause ozone depletion and warming.

In summary, large explosive volcanic eruptions have been observed throughout human history to cause global cooling of up to 0.6^{o}C for up to 3 years and can increment Earth into ice ages when occurring every decade or so. Voluminous extrusive eruptions of basalt lasting months to hundreds-of-thousands of years have been contemporaneous with major global warming of many degrees centigrade during eruptive periods throughout both human and geologic history. The balance between explosive and extrusive volcanism is determined by the motions of tectonic plates (Ward, 1995, 2009) and has a dominant effect on climate because both types of volcanic eruptions deplete ozone.

6 All volcanic eruptions deplete ozone

The longest continuous measurements of total column ozone have been made since 1927 at Arosa, Switzerland (46.8^{o}N, 9.7^{o}E, black line, Fig. 6) (Staehelin et al., 1998). The dashed grey line with blue data markers shows, for 1964 to 2009, the annual mean area-weighted total ozone deviation from the 1964 to 1980 means for northern mid-latitudes (30^{o}N to 60^{o}N) scaled from -8% at the bottom of the figure to 10% at the top (Douglass et al., 2011). Years of increasing or decreasing ozone are nearly identical at Arosa and for this area-weighted mean with small differences in amplitude. Thus the Arosa data provide a reasonable approximation for annual mean total column ozone throughout northern mid-latitudes since 1927.

Ozone at Arosa averaged 331 DU until 1974, fell 9.4% to 300 DU by 1993 and began generally rising again until 2011. The long-term decrease in ozone has been reliably associated with an increase in the concentration of anthropogenic tropospheric chlorine (green line, y-axis inverted) through chlorine catalysed destruction of ozone (Solomon, 1999). The resulting Montreal Protocol on Substances That Deplete the Ozone Layer was signed beginning in 1987, leading to phasing out the production of chlorofluorocarbons and hydrochloro-fluorocarbons and a decrease in tropospheric chlorine beginning in 1993. Long-term ozone concentrations are expected to return to late-1970's levels by 2040 (Solomon, 1999).

The lowest levels of annual mean total column ozone were observed in 1992 and 1993 following the 1991 eruption of Mt. Pinatubo (Kerr, 1993), the largest explosive eruption since 1912, and in 2011 and 2012 following the eruption of Eyjafjallajökull in 2010, one of the larger effusive eruptions of the past century. The size of an explosive volcanic eruption is typically measured using the logarithmic Volcanic Explosivity Index (VEI) based primarily on the volume of tephra erupted and the maximum height of the eruption column (Newhall and Self, 1982; Siebert et al., 2010). The size of effusive volcanic eruptions is best measured using the volume of magma extruded. Volcanoes labelled in red (Fig. 6) include all very large explosive volcanic eruptions with VEI ≥5, some VEI 3 and 4 extrusive eruptions in Iceland, and two explosive VEI 4 eruptions from volcanoes elsewhere that typically included substantial lava flows. All volcanic eruptions shown were followed a year later by a substantial decrease in annual mean total column ozone except the 1980 eruption in Washington state of Mt. St. Helens, an unusual blast of steam triggered by a landslide on the intruding volcanic plug (Druitt, 1992). Most other small volcanic eruptions since 1927 appear to cause similar changes in ozone, but the signal-to-noise ratios are too small to draw reasonable conclusions.

There is an increase in ozone the year of most of these eruptions compared to the previous year as discussed in more detail in Appendix B. There are also large peaks in annual mean total column ozone during years containing the three largest atmospheric nuclear tests labelled in black with yield in megatons (Fig. 6) (Wikipedia, 2013a; Johnston, 1977). The largest short-term peak in ozone was in 1940 and 1941 during the major territorial conquests of World War II. Any causal relationship is unclear. There is also a peak in 1998 during one of the largest El Niños in history but no obvious peak in 1982 and 1983 during an El Niño with a comparably large multivariate ENSO index (NOAA, 2013a), although the latter observation may have been complicated by the eruption of El Chichón in 1982. But the most consistent short-term changes in ozone in Fig. 6 are an apparent increase in ozone during the

year of a volcanic eruption followed by a much larger depletion during the next few years.

Pinatubo erupted in the Philippines on 15 June 1991 (VEI 6) followed closely by the eruption of Cerro Hudson in southern Chile on 12 August 1991 (VEI 5+). Annual mean ozone increased 3.9% in 1991 primarily between February 19 and 26 discussed in Appendix B. By 1993, annual mean ozone dropped 8.5% to 300 DU, the lowest level recorded by that time (Gleason et al., 1993; Angell, 1997b). Total column ozone was 11 to 17% below preceding years throughout Canada with a peak loss of 30% at ~16 km (Kerr et al., 1993). On average, total ozone decreased 8% in Europe, 5 to 6% in North America, Russia, and Asia but <2% in the tropics (Angell, 1997b). Following the 1982 eruptions of El Chichón in Mexico (VEI 5 and 4+), total ozone similarly decreased 5% in Europe, 3% in North America and Russia and <1% in the tropics (Angell, 1997b). Following the 1963 eruptions of Agung in Bali (VEI 5 and 4), total ozone fell 5% in Europe and Asia, 2% in North America, and <1% in the tropics (Angell, 1997b).

An even larger ozone anomaly in 2010 is associated with the 100-times less-explosive basaltic effusive eruption of Eyjafjallajökull in Iceland (VEI 4). A slightly larger (VEI 4) eruption of Grímsvötn, 140 km northeast of Eyjafjallajökull, occurred in May 2011, compounding the amount of ozone depletion during 2011 and 2012. The amplitudes of these short-term ozone anomalies since 1990 are larger than the amplitudes of earlier volcanic anomalies before the global rise in tropospheric chlorine (green line, y-axis inverted). Similar anomalies appear associated with the eruption of Hekla in Iceland (1970, VEI 3).

Following the eruption of Pinatubo, the lower troposphere warmed up to 3^{o}C during the winter throughout the more northerly parts of the northern continents (Robock, 2002), the parts with greater depletion of ozone. Related major changes in atmospheric chemistry are well documented by a 45% drop in total column NO_2 above Switzerland beginning five months after the Pinatubo eruption and returning to normal with an e-folding time of two years (De Mazière et al., 1998), a 40% decrease in NO_2 column observed above New Zealand (Johnston et al., 1992), and substantial increases in HNO_3 concentrations due to heterogeneous conversion of N_2O_5 (Coffey, 1996).

The observed ozone depletion (black line, Fig. 6) was accompanied by cooling of the stratosphere (purple line) occurring mostly “as two downward ‘steps’ coincident with the cessation of transient warming after the major volcanic eruptions of El Chichón and Mount Pinatubo” (Thompson and Solomon, 2009) and a similar downward step following the 1963 eruptions of Agung volcano (Randel, 2010).

Ozone depletion following volcanic eruptions has traditionally been explained by new aerosols formed in the lower stratosphere providing substantial new surfaces for heterogeneous chemical reactions to form ozone-destroying chlorine at cold temperatures in a polar vortex (Angell, 1997a). Yet water vapour (H_2O), the most voluminous gas erupted from volcanoes, is the primary source of OH radicals that catalytically destroy ozone in the stratosphere (Coffey, 1996; Anderson et al., 2012). Volcanoes also erupt megatons of halogens (Coffey, 1996), primarily chlorine and bromine (SPARC, 2009), and only one halogen molecule can destroy >100,000 molecules of ozone (Molina and Rowland, 1974). During explosive eruptions, many of these halogens appear to be removed immediately from the eruptive cloud in

condensed supercooled water (Tabazadeh and Turco, 1993). But extrusive, basaltic eruptions such as Eyjafjallajökull and Grímsvötn do not form significant eruption columns that remove halogens and that create aerosols in the stratosphere. They typically involve 10 to 100 times more volatiles per cubic kilometre of magma than explosive eruptions (Palais and Sigurdsson, 1989; Freda et al., 2005; Self et al., 1996). Ozone depletion is substantial within the plumes of erupting volcanoes; detailed observations imply that "the most likely cause for the observed rapid and sustained O_3 loss to be catalytic reactions with halogen, mainly bromine, radicals" (Vance et al., 2010). Recent observations have shown that even the plumes of quiescently degassing volcanoes are chemically very active, containing halogens that modelling shows cause ozone depletion (von Glasow, 2010). Between erupting many halogens and injecting large amounts of water into the stratosphere (Anderson et al., 2012), volcanoes appear to deplete ozone along many more chemical paths than attributed to anthropogenic chlorofluorocarbons.

Volcanic eruptions are typically followed a year later by ~6% depletion of ozone averaged throughout the year (Fig. 6). How do these short-term effects of volcanism compare to the longer-term effects of anthropogenic chlorofluorocarbons? The green line for chlorine is inverted and has been scaled so that the increase in anthropogenic tropospheric chlorine from 1965 to 1993 has approximately the same rate of change as the corresponding long-term decrease in ozone as expected by current theory. This visual fit suggests that depletion of ozone following the Pinatubo eruption (~20 DU) was twice as large as the depletion due to chlorofluorocarbons since 1960 (~10 DU) and that it takes more than a decade for ozone concentrations to return to pre-eruption levels.

In summary, large, explosive volcanic eruptions are well known to form sulphuric acid aerosols in the lower stratosphere that reflect, scatter, and absorb solar radiation, causing cooling at Earth's surface of up to 0.6^{o}C over three years. These explosive eruptions also deplete ozone causing warming that lasts 3 to 5 times longer than the aerosols, but the cooling effects of the aerosol predominate during the first three years except in winter/spring over northern continents when ozone depletion is particularly strong. The much less explosive and much more numerous basaltic extrusive eruptions such as Eyjafjallajökull and Grímsvötn as well as quiescently degassing volcanoes (von Glasow, 2010) do not form significant aerosols in the lower stratosphere so that ozone depletion and related warming dominate.

7 Ozone depletion was contemporaneous and co-located with record warming and drought in 2012 and 2013

Ozone, created primarily in the tropics, is moved in and above the Hadley cell upwards, then toward the poles and then downward into the lower stratosphere poleward of 30^{o} latitude (Fig. 4a) (Cordero et al., 2003). This Brewer-Dobson Circulation causes a minimum concentration of ozone in the tropics and an accumulation of ozone primarily in the winter hemisphere and especially in the northern hemisphere (Fig. 4b) (Fioletov, 2008). Increased ozone concentrations during the winter warm the lower stratosphere and thereby cool the troposphere. The greatest depletion of ozone from concentrations typical prior to 1950 occurs during these winter peaks.

The blue line in Fig. 7a shows the average monthly total column ozone measured above Toronto, Canada, averaged for the years 1961 through 1970 when anthropogenic tropospheric chlorine had only increased 16% from levels in 1925 towards peak levels in 1993 (green line, Fig. 6). The green line in Fig. 7a shows average monthly column ozone for 2009 when anthropogenic chlorine had decreased 9% from its peak value. Note that ozone depletion is greatest between December and May, the months of greatest warming throughout the northern hemisphere (Trenberth et al., 2007). The mean change in radiative forcing between the 1960s and 2009 caused by ozone depletion should be directly proportional to the area between the blue and green lines.

The solid red line includes both the increase in ozone during February preceding the first eruption of Eyjafjallajökull in March, 2010, discussed in Appendix B, and subsequent depletion. The dashed red line shows total ozone in 2011 including depletion due to Eyjafjallajökull and increases and decreases related to the eruption of Grímsvötn. The double red line shows ozone levels in 2012; the purple line for 2013. Note that from November 2011 through February 2012, the times when monthly maximum temperature records have been set throughout central North America (NOAA, 2012a), ozone has been depleted by as much as 14% below mean values in the 1960s.

The dashed black line in Fig. 7b shows the average for each year of the monthly mean total column ozone above Toronto averaged over five consecutive months from December through April; the dashed red line (y-axis inverted) shows the same average for monthly mean minimum temperatures. The solid lines are the same data smoothed using a 3-month symmetric running mean. A substantial decrease in ozone is typically but not always associated with an increase in minimum temperature except in 1992 to 1995 when aerosols in the lower stratosphere following the June, 1991, eruption of Pinatubo decreased radiation from Sun as much as 2.7±1.0 W m^{-2} during August and September (Minnis et al., 1993) decaying exponentially to negligible values by 1995. Note the extremely low ozone and high temperature in early 2012 (circled data points, lower right).

These data suggest that depletion of ozone due to the eruptions of Eyjafjallajökull in 2010 and Grímsvötn in 2011 supplemented anthropogenic depletion leading to extreme ozone depletion and to extreme warm temperatures and drought observed throughout the Great Plains of North America during late 2011 and 2012 (Karl et al., 2012) and to the highest sea surface temperatures ever recorded on the continental shelf off the northeastern United States during the first half of 2012 (NOAA, 2012b; Sallenger Jr et al., 2012). The Multivariate ENSO Index, on the other hand, shows only a transition from La Niña to moderate El Niño conditions in 2012 (NOAA, 2013a).

The drought of 2012 approached the intensity of the great Dust Bowl droughts of 1934 and 1936 (Brönnimann, 2009) when a highly unusual sequence of seven VEI 4 and 5 eruptions occurred from 1931 through 1933 in Indonesia, Japan, Kurile Islands, Kamchatka, Alaska, Guatemala, and Chile (Global Volcanism Program, 2013), providing at least a partial explanation for the well-known warming of mean northern hemispheric surface temperatures during the 1930s followed by cooling in the 1940s (red line, Fig. 8) (HadCRUT3nh, 2013).

On 12 July 2012 there was an extreme melt event across 98.6% of the Greenland ice sheet (Nghiem et al., 2012). Such melt events at high elevations in Greenland are extremely rare, last seen in 1889 and before that around 1200 (Clausen et al., 1988; Meese et al., 1994). The 1889 melting was coincident with a major El Niño (Chen et al., 2004) and the onset of major drought in 1889 from Mexico to Saskatchewan (Herweijer et al., 2007). These events followed the 1883 eruption of Krakatau (VEI 6), the 1886 eruption of Okataina (VEI 5), and several VEI 4 eruptions. These observations raise the possibility that the major El Niño in 1998 and associated warming might have been related to major ozone depletion (Fig. 6) following the eruptions of Pinatubo (VEI 6) and Cerro Hudson (VEI 5+) in 1991 after the cooling effects of the stratospheric aerosol had ended and compounded by three VEI 4 eruptions between 1992 and 1994.

Another possible relationship is that recent warming and drought were enhanced by the fact that November, 2011, had the largest number of sunspots per month since October, 2002 (NASA, 2013b), and ultraviolet insolation increases four to six times more than broadband irradiance during solar cycles (Haigh et al., 2010). In 1933 and 1934, however, the numbers of sunspots per month were relatively low until late in 1936.

These possible interrelationships before 2010 will need much more detailed study, but substantial depletion of ozone during 2011 and 2012 in mid-to-polar latitudes over North America does appear to be contemporaneous and co-located with both warming and drought in North America.

8 Ozone depletion was contemporaneous with 20th century warming

Annual mean surface temperatures in the northern hemisphere (red line, Fig. 8) (Rayner et al., 2006; HadCRUT3nh, 2013) increased during the 1930s, cooled during the 1940s, remained relatively constant until 1975, rose rapidly until 1998 with a net temperature increase of ~0.8^{o}C, and have remained relatively constant until 2011 (Trenberth, 2009; Knight et al., 2009). Other compilations of instrumental temperatures (Hansen et al., 2010; Smith et al., 2008) and analysis of 173 proxies for temperature since 1880 (Anderson et al., 2013) show similar trends.

Temperatures in the lower stratosphere (purple line, Fig. 6) decreased ~1.5^{o}C from 1958 to 1997 and have remained relatively constant since then. “Ozone depletion is believed to have caused the preponderance of the cooling in the lower stratosphere (15-25 km) altitude” but current models substantially underestimate the amplitude of this cooling and have trouble simulating the observed changes associated with volcanic eruptions in 1963, 1982, and 1991 (Thompson et al., 2012).

Concentrations of total tropospheric chlorine caused by anthropogenic chlorofluorocarbons (green line) increased rapidly from 1970, reached a peak in 1993 due to implementation of the Montreal Protocol and continue to decline slowly (Solomon, 1999).

Annual mean total column ozone (O_3, black line, y-axis inverted) fell rapidly from 1971 to 1995 and has been recovering slowly until volcanic eruptions in 2010 and 2011 (Staehelin et al., 1998). A slight delay after changes in tropospheric chlorine concentration is expected to give time for ozone to move to high latitudes where the

highest concentrations of ozone and the greatest depletion of ozone occur during winter (Figs. 4b and 7a).

The primary time delay in the atmospheric system involves the heat capacity of the ocean covering 71% of Earth. The observation in Fig. 8 that air temperatures above the ocean surface rose ~5 years after the decrease in ozone is in the range of calculations for a 3.5-year e-folding time for warming the ocean if the equilibrium temperature of Earth suddenly increased a small amount and a 10-year e-folding time taking into account an ocean with a 100-meter-thick mixed-layer (Hansen et al., 1985).

World ocean heat content (OHC, dashed purple line) increased from 1969 to 1980, remained relatively constant until 1990, and has been increasing ever since (Levitus et al., 2012). The time relationship between ocean heat content, volcanism, and annual total ozone is shown more clearly by the dashed red line in Fig. 6 where the ozone data have not been smoothed. The slow change in ocean heat content between 1980 and 1990, smoothed with a 5-year running mean, reflects the observed global cooling of up to 0.6^{o}C for up to three years following the eruptions of El Chichón (1982) and Pinatubo/Cerro Hudson (1991) (Domingues et al., 2008). Continued rise of ocean heat content since 1998, when temperatures levelled off, suggests that ocean heat content may be driven more by increased ultraviolet energy due to ozone depletion than by temperatures in the lowermost troposphere. In the last decade, about 30% of ocean warming has been below 700 metres (Balmaseda et al., 2013).

SO_2 emissions (dotted black line), 88% from burning fossil fuels, rose rapidly from 1950 until 1973 when concern over acid rain led to the addition of smokestack-scrubbers and other emission controls, as well as substitution of North Sea oil for coal in Europe (Smith et al., 2011; Klimont et al., 2013). The result was a 20% decrease in SO_2 emissions by 2002. Anthropogenic SO_2 emissions, primarily from northern Russia, Europe, United States, and southern Canada, led to the large deposits in ice cores in Greenland at time 0 (20th century) of what is labelled in Fig. 5 as volcanic sulphate. Between 2000 and 2008, emissions of SO_2 from China and India increased ~60% (Neely et al., 2013) but the 4 to 10% per year increase in stratospheric sulphate aerosols between 2000 and 2010 appears caused by small volcanic eruptions and not anthropogenic SO_2 (Neely et al., 2013).

The increase in atmospheric concentrations of CO_2 (blue line) (NOAA, 2013b) appears more closely related to the increase in ocean heat content than to an increase in surface temperature anomaly (red line, Fig. 8). The rate of increase in HadCRUT3nh temperatures nearly fell to zero in 1998 from ~0.27^{o}C per decade between 1985 and 1998 to 0.07±0.7^{o}C per decade between 1999 and 2008 (Knight et al., 2009) while CO_2 concentrations continued to increase at the same or slightly higher rate. The annual rate of increase in concentrations of CO_2 was <0.1 ppm/yr from 1938 to 1947 but began increasing to 0.7 ppm/yr by 1960 as concentrations of SO_2 were rapidly increasing. From 1976, however, by the time ocean heat content had begun increasing, the annual rate of increase of CO_2 doubled and even quadrupled to between 1.3 and 2.7 ppm/yr. Annual concentrations of CO_2 have increased every year since 1959 but the rate of increase dropped from 1.3 ppm/yr in 1990 to 0.7 in 1992 when global temperatures dropped and the increase in ocean heat content slowed following the eruption of Pinatubo in 1991 even though CO_2 was

the second most voluminous gas erupted after water vapour. Similar but smaller changes were observed associated with the 10-times smaller eruptions of Agung in 1963 and El Chichón in 1982. These observations suggest that the strong correlation between atmospheric temperatures and CO_2 concentrations going into and coming out of ice-age conditions (Petit et al., 1999; Siegenthaler et al., 2005; Siegenthaler et al., 2008) may primarily reflect the increase in solubility of CO_2 in a cooling ocean. From this perspective, CO_2 may be more a proxy for ocean temperature than a cause of increases in atmospheric temperatures (Appendix A).

The most surprising observation in Fig. 8 is that SO_2 emissions increased ~30 years before temperatures increased. There is little physical basis for explaining such a long time delay, so we might wonder whether SO_2 at concentrations of <50 ppbv (EPA, 2013; Cao et al., 2009) has any substantial effect on atmospheric temperatures. Studies related to the eruption of Pinatubo show that SO_2 injected into the stratosphere at concentrations in excess of 300 ppbm forms aerosols whose particle sizes grow large enough over months to reflect sunlight and cool Earth (Self et al., 1996). Substantial amounts of SO_2 in the more turbulent troposphere are not rapidly oxidized, travelling more than half way around the Earth in 8 to 12 days (Fiedler et al., 2009), and any aerosol formed in the troposphere has trouble growing to large enough particle sizes to scatter sunlight substantially.

Concentrations of other pollutants shown in Fig. 9 also increased ~30 years before warming. NO_X emissions (olive line), 58% from vehicles and 34% from fossil fuels (EPA, 2012), show a trend similar to SO_2 but with a slower decrease in vehicle pollution. Black carbon emissions (dashed black line) (Bond et al., 2007), the product of incomplete combustion, began increasing at rates similar to SO_2, dropped precipitously with improvements in diesel-engine design, first applied in this accounting in 1965 (Novakov, 2003), and levelled off by 2000 as emissions decreased in the West but increased in Asia.

Methane concentrations (green line) (Dlugokencky, 2010; Etheridge et al., 1998; Dlugokencky et al., 2009) increased gradually with emissions of other pollutants, reached a relatively constant rate of increase of ~14 ppb/year from 1955 to 1992, stopped increasing by 2006 and began increasing again at a rate of ~6 ppb/year in 2007 (Dlugokencky, 2010; Etheridge et al., 1998). The lifetime of methane is ~12 years, partially explaining the time lag. Methane concentrations are increased by fossil fuel use (Aydin et al., 2011), biomass burning, certain types of agriculture (Kai et al., 2011), and thawing of permafrost. Methane is removed from the atmosphere when oxidized by OH. Observed changes in OH concentrations may explain much of the observed changes in methane.

OH concentrations increase with increasing NO_X, tropospheric O_3, and sunlight, and decrease with increasing SO_2, carbon monoxide (CO), methane, and other pollutants it oxidizes. “A major pathway for production of OH radicals is the photolysis of ozone by solar UV-B” so that concentrations of OH increase with increasing frequency of photolysis (Rohrer and Berresheim, 2006). OH radicals react with tropospheric trace constituents typically within one second, making global concentrations of OH very difficult to observe and model, but modelling suggests they have decreased 9% since preindustrial times (Wang and Jacob, 1998). Formaldehyde (CH_2O) data from Greenland suggest OH concentrations may have decreased by as much as 30%

(Staffelbach et al., 1991). Detailed observations show a gradual decrease from 1980 to 2000 (Bousquet et al., 2005).

CO in the northern hemisphere increased 0.85%/year from 1950 to 1987 (Zander et al., 1989), decreased very slightly from 1988 (when detailed measurements began) to 2001, and increased slightly to 2005 (Duncan et al., 2007).

Concentrations of water vapour and ozone in the lowermost stratosphere increased until 2000 but began decreasing suddenly in 2001 (Randel et al., 2006; Solomon et al., 2010) when emissions of SO_2 stopped declining and began to increase again.

Tree ring density and thickness normally increase with temperature, but since the 1940s, they have decreased in northern forests while temperatures increased (D'Arrigo et al., 2008). SO_2 is well-known to stress and even kill trees (Keller, 1984; Manninen and Huttunen, 2000). When anthropogenic SO_2 levels began to decline in the early 1980s, wide-spread greening in northern regions was observed from satellites (Nemani et al., 2003).

All of these direct observations suggest that rapid increases in anthropogenic pollution since World War II do not appear to have the immediate influence on global temperatures implied by current computer-codes calculating the exchange of energy from radiation to matter and visa versa. All observations have been plotted on the same x-axis time scale with the y-axis adjusted so that both the mean values before 1965 and the peak values since 1998 are more or less lined up. Ultimately these data will need to be modelled to determine the quantitative interrelationships, but first current models need to be improved substantially to address the issues with radiation codes, with ozone, and with volcanoes described in this paper.

The purple dotted line (y-axis reversed) shows simulated annual clear-sky surface solar radiation (SSR) anomalies for mid-latitudes in the northern hemisphere calculated via current theory (Wild, 2009). The models predict that SSR decreased with increasing SO_2 and related pollution and increased with decreasing pollution. Note the rapid decreases in SSR for ~3 years following the large volcanic eruptions of El Chichón and Pinatubo. The blue dotted line (y-axis reversed), on the other hand, shows annual mean surface solar radiation observed at Stockholm (Wild, 2009). While SSR is likely to vary with regional differences in pollution, there is little similarity between long-term changes in theoretical and observed SSR especially prior to 1970. The radiation codes currently used by all models do not appear to be accurate.

9 Conclusions and courses of action

When the normal amount of ozone in the stratosphere is depleted, less solar ultraviolet energy is absorbed in the stratosphere, the stratosphere cools, the tropopause rises, and more ultraviolet energy reaches Earth where it is absorbed most efficiently in the oceans covering 71% of the surface. Temperature increase is proportional to energy increase, and, according to Planck's postulate, the energy contained in this ultraviolet radiation is 48 times the energy contained in infrared radiation absorbed most strongly by carbon dioxide.

The primary warming of the globe from 1970 to 1998 was caused by anthropogenic emissions of chlorofluorocarbons that last many decades in the atmosphere where

they are slowly converted in polar regions to chemically active chlorine compounds that caused ~3% depletion of ozone. The Montreal Protocol in 1989 led to reductions of these emissions by 1992, but they are not expected to return to 1970 levels until 2040.

Meanwhile the large, explosive eruption of Pinatubo volcano in 1991 further depleted ozone nearly 6% decaying back to normal within approximately ten years. While the stratospheric aerosols caused by this explosive eruption cooled Earth for ~3 years, related ozone depletion caused warming over northern continents during the winters of 1991 and 1992 and ultimately net warming globally. Mean surface temperatures have remained relatively constant since 1998, but ocean heat content continues to rise probably due to the long-term anthropogenic depletion of ozone. Eruptions of small, effusive, basaltic volcanoes in Iceland during 2010 and 2011 each caused short-term depletion of ozone by 6% causing major warming and drought best documented in central North America during 2012 and 2013 and in ocean temperatures between north-eastern North America and Europe.

Concentrations of ozone and gases whose chemistry relates to ozone change radically over timeframes from hours, to seasons, to millennia along the edges of the polar vortex in the Antarctic but especially along the rapidly-changing vortex in the Arctic. Observed short-term changes appear closely related to changes in weather, providing a direct link between climate and weather that needs to be studied in considerably more detail.

Observations and theory suggest that climate is an equilibrium influenced primarily by changes in total column ozone, more than 90% of which resides in the lower stratosphere. Humans can best influence climate change by eliminating emissions of all substances that deplete stratospheric ozone and by seeking ways to remove any of these substances still in the atmosphere or placed in the atmosphere by natural processes. The Montreal Protocol has been very effective in reducing the quantities of these substances produced, yet some are still available on the black market.

Observations and theory show pollution does not have much effect on global warming unless ozone is depleted. Pollution does have major effects on health, has been reduced substantially in most developed countries, and needs to be reduced most urgently in China, India, and other countries with rapid growth in energy consumption. Ozone produced in the lower troposphere as a result of pollution is very toxic and its concentrations need to be reduced world-wide.

Observations and theory show absorption by CO_2 and other greenhouse gases does not have the substantial effect on global warming currently assumed. Ozone depletion provides a much more direct explanation for the timing and location of temperature changes around the world. Simply reducing CO_2 emissions is unlikely to reduce global warming but it is likely to reduce ocean acidification.

Appendix A: More problems with greenhouse gases

CO_2 concentrations have increased and decreased at nearly the same time as global temperatures during the 20th century (Fig. 8), during ice ages (Siegenthaler et al., 2005; Lüthi et al., 2008), and throughout the Phanerozoic (Royer, 2006). Many people see this as confirmation of greenhouse gas theory. But contemporaneity is not proof of cause. Most detailed studies suggest that CO_2 levels before the 20th

century rose after temperature increased (Fischer et al., 1999; Monnin et al., 2001; Caillon et al., 2003; Stott et al., 2007; Tachikawa et al., 2009; Siegenthaler et al., 2005; Pedro et al., 2012) although others disagree (Shakun et al., 2012; Parrenin et al., 2013) pointing out that air is not trapped in snow until buried 50 to 120 meters, which can take hundreds of years in the Arctic and thousands of years in the Antarctic.

From 1998 to 2008, temperatures remained fairly constant (Knight et al., 2009) while ocean heat content and concentrations of CO_2 continued to increase (Fig. 8). The solubility of CO_2 in water is well known to decrease with increasing water temperature just as a carbonated beverage loses CO_2 as it warms. Thus, atmospheric concentrations of CO_2 appear to be more related to ocean heat content and enhanced wind-driven upwelling around Antarctica (Anderson et al., 2009) than to global mean temperatures just above Earth's surface.

The sensitivity of climate to a doubling of CO_2 is not observed in the laboratory nor in nature, it is calculated assuming that all warming during a certain period of time was caused by greenhouse gases (PALEOSENS Project Members, 2012). On the contrary, I have shown that ozone depletion plays a substantial role in warming Earth's surface.

CO_2 concentrations during the Pliocene climate optimum around 4 million years ago were as much as 100 ppm less than today while climate had "substantially lower meridional and zonal temperature gradients but similar maximum ocean temperatures" (Fedorov et al., 2013). These large structural changes in climate cannot be explained by current Earth system models implying that either climate went over some threshold or was cooled by mechanisms other than CO_2 (Fedorov et al., 2013).

High-resolution paleoclimatic studies in the Late Miocene (LaRiviere et al., 2012) as well as the existence of glaciation in Devonian and Permian-Triassic times when CO_2 concentrations appear to have been >10 and >5 times preindustrial values respectively (Berner, 2009) suggest that increased CO_2 concentrations are not a primary cause of global warming.

The width of the tropical belt widened 2^o to 5^o in latitude since 1979 (Seidel et al., 2008). Expansion in the Southern Hemisphere has been attributed to ozone depletion (Polvani et al., 2011) and "recent Northern Hemisphere tropical expansion is driven mainly by black carbon and tropospheric ozone, with greenhouse gases playing a smaller part" (Allen et al., 2012).

Absorption by any gas of radiant energy not energetic enough to cause photodissociation does not appear to cause much warming (Fig. 8 and 9). Even the greatest concentrations of ozone in the stratosphere are not at the levels of the greatest heating.

Periods of global warming typically start abruptly and are contemporaneous with major increases in volcanism at the end of the last ice age, during the 24 sudden Dansgaard-Oeschger warming events over the past 250,000 years (Dansgaard et al., 1993) (Ward, 2009), during the opening of the Greenland-Norwegian Sea in the early Eocene (Storey et al., 2007), and during the largest mass extinctions over the past 360 million years (Ward, 2009). Volcanic eruptions provide a clear explanation for sudden change while "a close examination of paleoclimatic data and modelling

results does not show adequate support for many of the widely accepted explanations for abrupt climate change" (Rashid et al., 2011) including freshwater forcing, changes in sea ice extent, and tropical forcing (Clement and Peterson, 2008).

Since the concentration of CO_2 is essentially homogeneous throughout the globe and increases monotonically with time, it is very difficult to explain how changes in CO_2 concentrations can cause the clearly observed amplification of warming in Polar Regions (Serreze and Barry, 2011) and why the greatest warming occurs during mid-to-late winter.

Climate models that utilize CO_2 as a primary driver of temperature increase have overestimated global warming since 1998 (Trenberth and Fasullo, 2010; Hansen et al., 2005) and are probably overestimating warming in future decades. Their links to regional climate are also tenuous (Kerr, 2013).

Appendix B: Apparent increases in ozone before volcanic eruptions

Annual total column ozone observed at Arosa increased 12 DU (4%) in 1991, the year Pinatubo and Cerro Hudson erupted, but decreased 28 DU (8%) by 1993 (Fig. 6). Similarly ozone increased 14 DU (4%) in 2010 when Eyjafjallajökull erupted but decreased 28 DU (8%) in 2011. Other volcanic eruptions shown in Fig. 6 are also contemporaneous with a modest increase in ozone followed the next year by a decrease of at least twice as much.

The ozone increase in 2010 occurred primarily between 19 February and 26 February, ~4 weeks before the first extrusive flank eruption of basalt from 20 March to 12 April and ~7 weeks before the main explosive eruption of trachyandesite on 14 April. Fig. B1 shows that total ozone northeast of Iceland increased to more than 550 DU on 19 February over a background of ~325 DU, an increase of ~70% (Environment Canada, 2013a). The deviation of total ozone over the period from 21 February to 28 February increased 45% compared to mean levels from 1978 thru 1988 (Environment Canada, 2013a). The sudden onset of these emissions is shown clearly in an animation of daily ozone maps from 1 December 2009 to 30 April 2010 (Ward, 2013b).

At Eyjafjallajökull, seismic activity and deformation began in December 2009, "explained by a single horizontal sill inflating at a depth of 4.0 to 5.9 km under the south-eastern flank of the volcano" (Sigmundsson et al., 2010). Deformation increased exponentially in February (Fig. B2), suggesting a major change in pressure conditions within the system by 4 March. Thus a substantial release of gas from the top of the magma body is highly likely to have occurred in late February as the roof of the intrusion fractured to the surface.

It is conceivable that oxygen fugacity in magma is sufficient to concentrate oxygen gas in the very high temperature (high energy) environment at the top of a magma body where ozone could be formed and then released when fractures first propagate to the surface. But oxygen and ozone are not likely volcanic gases because magma typically has a reduced oxidation state**.**

Sulphur dioxide (SO_2) is a primary gas emitted from high-temperature fumaroles. SO_2 absorbs ultraviolet solar radiation strongly at the same wavelengths as ozone (Fig. 3)

and is known to affect ozone measurements in urban areas such as Uccle, just outside of Brussels, Belgium (De Muer and De Backer, 1992). SO_2 is colourless so that its release from high-temperature fumaroles in the vicinity of the extrusive eruption that began on 20 March would have gone unnoticed if substantial water vapour was not included. There were no instruments in the vicinity to detect either SO_2 or ozone. But satellite data are normally sufficient to distinguish ozone from SO_2. Local farmers did note unusual melting of snow near high temperature fumaroles "months" before the eruption of Hekla in south Iceland on 5 May 1970 (Thorarinsson and Sigvaldason, 1972; Thorarinsson, 1970).

Another possibility is that high-temperature (high-energy) gases from basaltic magma (1300 to 1400^{o}C) (Lee et al., 2009) may interact in some way with water released from the magma, with ground water, or even with atmospheric water vapour to split oxygen atoms and form ozone. Magmatic high-temperature gases might also interact with volatile organic compounds or nitrogen compounds or gases to form ozone catalytically.

Yet another possibility is that the ozone was generated by rock fracture as the gases at the top of the magma broke to the surface. Crushing and grinding small samples of igneous and metamorphic rocks at atmospheric pressure in the laboratory generated up to 10 ppm ozone apparently "formed by exoelectrons emitted by high electric fields, resulting from charge separation during fracture" (Baragiola et al., 2011).

Mt. Pinatubo in the Philippines showed signs of reawakening with a group of felt earthquakes on 15 March 1991, the first steam explosions on 2 April, first eruption on 12 June, and the main eruption on 15 June. Ozone anomalies >550 DU, a 40% increase, occurred from 20 to 22 February 1991 at 44 to 58^{o}N, 115 to 140^{o}E (Fig. B3). The winter-time Brewer-Dobson circulation (Fig. 4a) is thought to move ozone and related gases from the latitude of Pinatubo (15.1^{o}N, 120.4^{o}E) up into the stratosphere, northward, and then downward north of 40^{o}N (Cordero et al., 2003). The sudden onset of these emissions is shown clearly in an animation of daily ozone maps for the northern hemisphere from 1 January 1991 to 10 May 1991 (Ward, 2013a). The upward motion of the Brewer-Dobson circulation in the tropics is thought to move normally at a rate of 20 to 30 metres per day (Cordero et al., 2003), but the heat of volcanic gases might increase that rate substantially.

Similar anomalies occurred over Hudson's Bay, Canada, at 60 to 70^{o}N from 26 February to 3 March, 1991, with no obvious spatial relationship to any volcano. These large ozone anomalies are most common during the winter (Fig. 4b), north of 60^{o}N, and they may be related to sudden stratospheric warming in specific regions (Waugh and Polvani, 2010).

The contemporaneity of some of these large ozone anomalies with pre-eruption intrusion could be coincidence. Considerable work is needed to prove any causal relationship. Ozone emission prior to volcanic eruptions would provide a good explanation for why the Great Oxidation Event 2.45 to 2.32 billion years before present was contemporaneous with the first known prodigious sub-aerial emissions of magma (Kump and Barley, 2007; Campbell and Allen, 2008; Kump et al., 2005).

Appendix C: What is electromagnetic radiation?

Climate is driven primarily by electromagnetic radiation (EMR) from Sun; climate change appears to occur primarily when more or less than normal amounts of solar energy are either absorbed or reflected by Earth's atmosphere changing the amount of energy reaching Earth's surface. What physically is EMR and how is it absorbed and reflected? Let's use the word light as shorthand for the much broader spectrum of EMR because we all have good physical intuition about light, because brightness is more intuitive than spectral amount, because the physics should be similar even though energy varies from less than 0.001 eV for the far-infrared to 2 or 3 eV for visible light, to more than 100 eV for the extreme ultraviolet, and because visible and near ultraviolet light play the primary role in heating Earth.

At any point in space, in a gas such as air, in a liquid, or in a translucent solid, light consists of a spectrum of frequencies (colours) where each frequency can be thought of as having spectral amount (brightness). This spectrum appears to travel the shortest distance between source and receiver, a straight line that we think of as a ray. When we look at colourful fall foliage, for example, each molecule or cell of everything we can see absorbs most radiation received from Sun and is warmed much like a pot on a stove. But the molecules or cells responsible for colour are caused to resonate, radiating a very narrow frequency spectrum. This radiation has a brightness determined by the brightness of the light illuminating matter. The brightness goes to zero as the amount of incoming light goes to zero, causing the molecule to no longer radiate visible frequencies bright enough to see, although the molecule continues to radiate infrared frequencies based on the temperature of the matter that it is part of. The radiation from each molecule received by our eyes, photographic film, or the CMOS sensor of a digital camera, for example, causes a photochemical reaction and the amount of that reaction is defined by the spectral amount (brightness) received at that specific frequency. Our field of view is made up of so many of these "rays" that we can resolve the intricacies of colour with very high resolution, yet these rays of light do not interfere with each other until they interact with matter. We take all this for granted, but it feels like "spooky interaction at a distance," Einstein's description of quantum entanglement. The energy of oscillation in one piece of matter influences the energy of oscillation in another piece of matter at an arbitrarily large distance separated by a gas such as air or by the vacuum of space. This simple "entanglement" is a physical property of an electromagnetic field. Quantum entanglement, even at speeds much greater than the velocity of light, has taken on far more complicated mathematical properties that are actively debated through the different interpretations prevalent in quantum mechanics.

Light illuminates matter, but light itself is not visible, it is dark, until it interacts with matter. Given that Earth receives less than 5×10^{-8} % of Sun's radiation, there must be a lot of dark energy in space that changes in time only if the rate of conversion of mass to energy in stars and elsewhere changes or locally as it interacts with matter, such as in the shadow behind a planet.

The widespread existence of dark energy suggests that the medium light travels in is light itself, i.e. there is an electromagnetic field located everywhere that permeates space, atmospheres, and matter in three dimensions. The physical properties of this field vary in time if the sources of energy vary. The spectral amount decreases proportional to one over the square of the distance from the source. Energy in the

form of frequency of oscillation appears to radiate outward from matter, travelling through this field along what is thought of as a straight line from source to receiver, although light rays can be bent very slightly by gravity, currently thought of as distortions in spacetime (Einstein, 1905b), and more strongly as they interact directly with matter. Energy is either extracted from this field by matter or the presence of matter changes the local physical properties of this field.

Planck's postulate (E=hv) says that light is simply energy in the form of frequency (cycles per second) whose existence seems to depend on the continual interaction between an electric field and a magnetic field, suggesting that what we think of as the velocity of light must be related to the rate that an electric field can induce a magnetic field, can induce an electric field, ad infinitum. There is no known medium (luminiferous aether) in space and there are no physical observations that show that light in space is either a wave or a particle, that it has wavelength or mass, because there can be no observation until light interacts with matter.

Light can travel inter-galactic distances without any change in frequency (except Doppler effects) and thus without any loss of energy, even though light diverges so that the amount of light, the brightness, is inversely proportional to the square of the distance from the centre of the source to the receiver. Thus for light in space, the energy contained in light and the amount of light (brightness) are separate variables commonly multiplied together in order to determine spectral radiance. This is distinctly different from the energy contained in waves within matter where the wave energy works against the bonds holding matter together so that energy at a given location is proportional to the square of the amplitude of the wave at that location. Light does not travel in space in exactly the same way that waves travel in matter, although light is observed to interact with matter in a wavelike manner. Thinking of light in space as having the physical property of wavelength may be very misleading.

Thus light might be described most precisely as field-particle-wave triality or vacuum-gas-solid triality to emphasize that the physical properties of light are different in space, atmospheres, and matter. In the vacuum of space, light is an energy field extending in three dimensions, affecting the behavior of matter in the presence of the field. The frequencies of light do not change over galactic distances except when there is motion between source and receiver, but the spectral amount is inversely proportional to the distance between source and receiver squared. Light from one source does not interfere with light from a separate source except in the presence of matter.

Light travels similarly through a gas such as air except some of the molecules of gas absorb certain frequencies of light in a particle-like manner. Each degree of freedom of motion among and within atomic components of a gas molecule resonates at its natural harmonic frequencies, extracting spectral amount at those frequencies from the light field, adding the energy to the molecule. The energy absorbed is along very narrow spectral lines (Rothman et al., 2009), implying high-Q classical sympathetic resonance perhaps similar to that observed when undamped strings of a piano resonate to specific frequencies of sound in the room. The spectral components of the energy absorbed are determined by the physical properties of the molecule. Energy absorbed through rotational and vibrational transitions is shared among surrounding atoms/molecules via collisions. Energy absorbed through electronic transitions typically causes what we think of as an electron to resonate at a higher

frequency (energy) similar to overtones on a vibrating string and this energy can be re-radiated typically through fluorescence when the atom/molecule returns to ground state often initiated by a collision. When these higher energy states are energetic enough, they can cause dissociation and even ionization, destroying the molecule.

The net energy transferred from the field to the gas molecule can be viewed as spectral amount for each frequency times Planck's E=hv (Planck, 1901) integrated across all frequencies, or, for simplicity, Einstein's light quantum (Einstein, 1905a), or Lewis's photon (Lewis, 1926), but the detailed nature of this energy is determined by the physical characteristics of the receiver, not the physical characteristics of the source. Therefore, it does not make physical sense to talk of photons propagating from the source. The photon is a very useful mathematical concept central to quantum mechanics that is shorthand for a complex distribution of frequencies (energies and amounts) transferred from an electromagnetic field to matter.

Atoms and molecules constituting a gas can be thought of as similar to radio antennas tuned to very specific frequencies. Each has a different orientation so that each responds slightly differently to the surrounding electromagnetic field. If we knew all the details about the state of every molecule and atom and the state of the field, we could determine which molecules will interact when and how with the field. But this is impractical given the very large number of atoms/molecules involved leading to the statistical nature of quantum mechanics.

When light interacts with matter, defined as an assemblage of atoms and molecules bound by attractive forces, it can be reflected, refracted, diffracted, polarized, dispersed, focussed, and/or attenuated because the energy in light works against the bonds holding matter together. The oscillations of light when interacting with matter cause waves in matter whose properties are determined by the nature of the matter such as the index of refraction, thought of as the ratio of the velocity of light in space to the velocity of light in matter. Light is attenuated in matter showing that energy and amount are now intermixed. Light in space and typically in air can be split by matter in a double-slit experiment (Young, 1802) where the width and spacing of the slits are small, causing the two rays to interfere, but rays from different sources of light do not interact until they both encounter the same piece of matter.

Sound, on the other hand, travels in air as compressional waves with a spectrum of frequencies emitted by oscillations at the source that cause the hair cells in the cochlea of the inner ear to resonate. The frequencies of sound do not change with distance and direction, except for Doppler effects, but spectral amounts from different sources are combined within air and are attenuated as the wave front spreads and as energy is absorbed by air, especially in the high frequencies.

Energy fields may be as large as the universe or as small as an electron or the fields that hold parts of atoms together. The diameter of a hydrogen atom is 145,000 times larger than the diameter of its nucleus. The vast majority of any atom is an energy field that we describe in terms of electrons and that de Broglie (1929) suggested consists of "stationary" waves in order to include "the concept of periodicity" (frequency). One could argue that everything consists of combinations of fields and the tiny components of matter, and that time (change) is made possible by the conversion of energy to matter and the conversion of matter to energy.

Natural scientists have debated since the time of Ancient Greece whether the energy contained in electromagnetic radiation (light) travels as waves or particles. By 1900,

most physicists thought that radiation travelled as waves according to Maxwell's equations (Maxwell, 1873) as demonstrated by Young's famous double-slit experiment (Young, 1802), but they could not decide what type of matter these waves travelled in. Planck's quantization of energy (E=hv) and Einstein's light quantum led to the development of quantum electrodynamics (QED) based on the wave-particle duality of electromagnetic radiation emitted by an ensemble of harmonic oscillators. QED is arguably the most successful mathematical theory in physics in terms of explaining and predicting observations, but it is non-deterministic and leads to many concepts that do not make physical sense, something that plagued Planck and Einstein for the rest of their lives. Light in space does not have the physical properties of wavelength or mass. Recognizing that electromagnetic radiation is simply a spectrum of frequencies (energies) that induces particle-like behaviour in atoms/molecules of gas and wave-like behaviour in matter is likely to make QED more deterministic, give us more physical insight into many of its conclusions, and bring us closer to understanding Nature.

Acknowledgements

Thanks to Johannes Staehelin and Rene Stuebi for updates to the ozone data from Arosa and to Vidali Fioletov for access to preliminary ozone data from Toronto. Thanks to Huiming Bao, James Bjorken, Terrance Gerlach, Peter Giles, Zach Hall, William Happer, George Helz, David Laing, Bertram Raynes, and Adrienne Ward for critical comments and especially to Michael MacCracken and Peter Molnar for critical reviews of many drafts over many years. Reviews that challenged many of my findings have been particularly useful. Thanks to the many contributors to Wikipedia for making knowledge so accessible.

References

ACRIM: Total Solar Irradiance (TSI) Monitoring: www.acrim.com/index.htm, 2013.

Allen, R. J., Sherwood, S. C., Norris, J. R., and Zender, C. S.: Recent Northern Hemisphere tropical expansion primarily driven by black carbon and tropospheric ozone, Nature, 485, 350-354, 10.1038/nature11097, 2012.

Andersen, S., and Knudsen, B.: The influence of polar vortex ozone depletion on NH mid-latitude ozone trends in spring, Atmos. Chem. Phys., 6, 2837-2845, 10.5194/acp-6-2837-2006, 2006.

Anderson, D. M., Mauk, E. M., Wahl, E. R., Morrill, C., Wagner, A. J., Easterling, D., and Rutishauser, T.: Global warming in an independent record of the past 130 years, Geophys. Res. Lett., 40, 1-5, 10.1029/2012GL054271, 2013.

Anderson, J. G., Wilmouth, D. M., Smith, J. B., and Sayres, D. S.: UV dosage levels in summer: Increased risk of ozone loss from convectively injected water vapor, Science, 337, 835-839, 10.1126/science.1222978, 2012.

Anderson, R. F., Ali, S., Bradtmiller, L. I., Nielsen, S. H., Fleisher, M. Q., Anderson, B. E., and Burckle, L. H.: Wind-driven upwelling in the Southern Ocean and the deglacial rise in atmospheric CO_2, Science, 323, 1443-1448, 10.1126/science.1167441, 2009.

Angell, J. K.: Stratospheric warming due to Agung, El Chichón, and Pinatubo taking into account the quasi-biennial oscillation, J. Geophys. Res., 102, 9479–9486, 10.1029/96JD03588, 1997a.

Angell, J. K.: Estimated impact of Agung, El Chichon and Pinatubo volcanic eruptions on global and regional total ozone after adjustment for the QBO, Geophys. Res. Lett., 24, 647–650, 10.1029/97GL00544, 1997b.

Asano, S.: Estimation of the size distribution of Pinatubo volcanic dust from Bishop's ring simulations, Geophys. Res. Lett., 20, 447-450, 10.1029/93GL00512, 1993.

Aydin, M., Verhulst, K. R., Saltzman, E. S., Battle, M. O., Montzka, S. A., Blake, D. R., Tang, Q., and Prather, M. J.: Recent decreases in fossil-fuel emissions of ethane and methane derived from firn air, Nature, 476, 198-201, 10.1038/nature10352, 2011.

Balmaseda, M. A., Trenberth, K. E., and Källén, E.: Distinctive climate signals in reanalysis of global ocean heat content, Geophys. Res. Lett., 40, 50382, 10.1002/grl.50382, 2013.

Baragiola, R. A., Dukes, C. A., and Hedges, D.: Ozone generation by rock fracture: Earthquake early warning?, Applied Physics Letters, 99, 204101, 2011.

Barrie, L., Hoff, R., and Daggupaty, S.: The influence of mid-latitudinal pollution sources on haze in the Canadian Arctic, Atmos. Environ., 15, 1407-1419, 10.1016/0004-6981(81)90347-4, 1981.

Beerling, D. J.: The Emerald Planet: How plants changed Earth's history, Oxford University Press, Oxford ; New York, xvi, 288 pp., 2007.

Berner, R. A.: Phanerozoic atmospheric oxygen: New results using the GEOCARBSULF model, Am. J. Sci., 309, 603-606, 10.2475/07.2009.03, 2009.

Bijl, P. K., Schouten, S., Sluijs, A., Reichart, G. J., Zachos, J. C., and Brinkhuis, H.: Early Palaeogene temperature evolution of the southwest Pacific Ocean, Nature, 461, 776-779, 10.1038/nature08399, 2009.

Black, B. A., Elkins-Tanton, L. T., Rowe, M. C., and Peate, I. U.: Magnitude and consequences of volatile release from the Siberian Traps, Earth Planet. Sci. Lett., 317, 363-373, 10.1016/j.epsl.2011.12.001, 2012.

Bluth, G. J. S., Doiron, S. D., Schnetzler, C. C., Krueger, A. J., and Walter, L. S.: Global tracking of the SO_2 clouds from the June, 1991 Mount Pinatubo eruptions, Geophys. Res. Lett., 19, 151-154, 10.1029/91GL02792, 1992.

Bond, T. C., Bhardwaj, E., Dong, R., Jogani, R., Jung, S., Roden, C., Streets, D. G., and Trautmann, N. M.: Historical emissions of black and organic carbon aerosol from energy-related combustion, 1850–2000, Global Biogeochem. Cycles, 21, GB2018, 10.1029/2006gb002840, 2007.

Bousquet, P., Hauglustaine, D. A., Peylin, P., Carouge, C., and Ciais, P.: Two decades of OH variability as inferred by an inversion of atmospheric transport and chemistry of methyl chloroform, Atmos. Chem. Phys., 5, 1679-1731, 10.5194/acp-5-2635-2005, 2005.

Bromwich, D. H., Nicolas, J. P., Monaghan, A. J., Lazzara, M. A., Keller, L. M., Weidner, G. A., and Wilson, A. B.: Central West Antarctica among the most rapidly warming regions on Earth, Nature Geosci., 6, 139-145, 10.1038/ngeo1671, 2013.

Brönnimann, S.: Early twentieth-century warming, Nature Geosci., 2, 735-736, 10.1038/ngeo670, 2009.

Bureau, H., Keppler, H., and Métrich, N.: Volcanic degassing of bromine and iodine: experimental fluid/melt partitioning data and applications to stratospheric chemistry, Earth Planet. Sci. Lett., 183, 51-60, 10.1016/S0012-821X(00)00258-2, 2000.

Caillon, N., Severinghaus, J. P., Jouzel, J., Barnola, J. M., Kang, J., and Lipenkov, V. Y.: Timing of atmospheric CO_2 and Antarctic temperature changes across termination III, Science, 299, 1728-1731, 10.1126/science.1078758, 2003.

Campbell, I. H., and Allen, C. M.: Formation of supercontinents linked to increases in atmospheric oxygen, Nature Geosci., 1, 554-558, 10.1038/ngeo259, 2008.

Cao, J., Garbaccio, R., and Ho, M. S.: China's 11th five-year plan and the environment: Reducing SO_2 emissions, Rev. Environ. Econ. Policy, 3, 231-250, 10.1093/reep/rep006, 2009.

Chen, D., Cane, M. A., Kaplan, A., Zebiak, S. E., and Huang, D.: Predictability of El Niño over the past 148 years, Nature, 428, 733-736, 10.1038/nature02439, 2004.

Christiansen, R. L.: The Quaternary and Pliocene Yellowstone Plateau volcanic field of Wyoming, Idaho and Montana, U.S. Geol. Surv. Prof. Pap., 729, 146 pp., 2001.

Clarke, A., Murphy, E. J., Meredith, M. P., King, J. C., Peck, L. S., Barnes, D. K. A., and Smith, R. C.: Climate change and the marine ecosystem of the western Antarctic Peninsula, Phil. Trans. R. Soc. London, Ser. B, 362, 149-166, 10.1098/rstb.2006.1958, 2007.

Clausen, H., Gundestrup, N., Johnsen, S., Bindschadler, R., and Zwally, J.: Glaciological investigations in the Crete area, central Greenland: A search for a new deep-drilling site, Ann. Glaciol., 10, 10-15, 1988.

Clement, A. C., and Peterson, L. C.: Mechanisms of abrupt climate change of the last glacial period, Rev. Geophys., 46, 1-39, 10.1029/2006RG000204, 2008.

Cofala, J., Rafaj, P., Schöpp, W., Klimont, Z., and Amann, M.: Emissions of air pollutants for the World Energy Outlook 2009 Energy scenarios: www.iiasa.ac.at/publication/more_XO-09-056.php, 2009.

Coffey, M. T.: Observations of the impact of volcanic activity on stratospheric chemistry, J. Geophys. Res., 101, 6767–6780, 10.1029/95JD03763, 1996.

Comiso, J. C.: Arctic warming signals from satellite observations, Weather, 61, 70-76, 10.1256/wea.222.05, 2006.

Cordero, E., Newman, P. A., Weaver, C., and Fleming, E.: Chapter 6 Section 3: The Brewer-Dobson Circulation, in: Stratospheric Ozone: An Electronic Textbook, www.ccpo.odu.edu/~lizsmith/SEES/ozone/class/Chap_6/index.htm, 2003.

Courtillot, V. E., and Renne, P. R.: On the ages of flood basalt events, C.R. Geosci., 335, 113-140, 10.1016/s1631-0713(03)00006-3, 2003.

CRUTEM4: http://www.cru.uea.ac.uk/cru/data/temperature/, 2013.

D'Arrigo, R., Wilson, R., Liepert, B., and Cherubini, P.: On the 'divergence problem' in northern forests: a review of the tree-ring evidence and possible causes, Global Planet. Change, 60, 289-305, 10.1016/j.gloplacha.2007.03.004, 2008.

Dansgaard, W., Johnsen, S. J., Clausen, H. B., Dahl-Jensen, D., Gundestrup, N. S., Hammer, C. U., Hvidberg, C. S., Steffensen, J. P., Sveinbjörnsdottir, A. E., Jouzel, J., and Bond, G.: Evidence for general instability of past climate from a 250-kyr ice-core record, Nature, 364, 218 - 220, 10.1038/364218a0, 1993.

de Broglie, L.: The wave nature of the electron: www.nobelprize.org/nobel_prizes/physics/laureates/1929/broglie-lecture.pdf, 1929.

De Mazière, M., Van Roozendael, M., Hermans, C., Simon, P. C., Demoulin, P., Roland, G., and Zander, R.: Quantitative evaluation of the post–Mount Pinatubo NO_2 reduction and recovery, based on 10 years of Fourier transform infrared and UV-visible spectroscopic measurements at Jungfraujoch, J. Geophys. Res., 103, 10849-10858, 10.1029/97JD03362, 1998.

De Muer, D., and De Backer, H.: Revision of 20 years of Dobson total ozone data at Uccle (Belgium): Fictitious Dobson total ozone trends induced by sulfur dioxide trends, J. Geophys. Res., 97, 5921-5937, 10.1029/91JD03164, 1992.

DeMore, W., Sander, S., Golden, D., Hampson, R., Kurylo, M., Howard, C., Ravishankara, A., Kolb, C., and Molina, M.: Chemical kinetics and photochemical data for use in stratospheric modeling: www.archive.org/details/nasa_techdoc_19970037557, 1997.

Derksen, C., and Brown, R.: Spring snow cover extent reductions in the 2008-2012 period exceeding climate model projections, Geophys. Res. Lett., 39, L19504, 10.1029/2012GL053387, 2012.

Deshler, T., Johnson, B. J., and Rozier, W. R.: Balloonborne measurements of Pinatubo aerosol during 1991 and 1992 at 41°N: vertical profiles, size distribution, and volatility, Geophys. Res. Lett., 20, 1435-1438, 10.1029/93GL01337, 1993.

Dlugokencky, E. J., Bruhwiler, L., White, J. W. C., Emmons, L. K., Novelli, P. C., Montzka, S. A., Masarie, K. A., Lang, P. M., Crotwell, A. M., Miller, J. B., and Gatti, L. V.: Observational constraints on recent increases in the atmospheric CH_4 burden, Geophys. Res. Lett., 36, L18803, 10.1029/2009gl039780, 2009.

Dlugokencky, E. J.: Carbon dioxide, nitrous oxide, methane, CFC-12, CFC-11: www.esrl.noaa.gov/gmd/aggi/aggi_2010.fig2.png, 2010.

Domingues, C. M., Church, J. A., White, N. J., Gleckler, P. J., Wijffels, S. E., Barker, P. M., and Dunn, J. R.: Improved estimates of upper-ocean warming and multi-decadal sea-level rise, Nature, 453, 1090-1093, 10.1038/nature07080, 2008.

Douglass, A., Fioletov, V., Godin-Beekmann, S., Müller, R., Stolarski, R., Webb, A., Arola, A., Burkholder, J., Burrows, J., and Chipperfield, M.: Chapter 2: Stratospheric Ozone and Surface Ultraviolet Radiation, in: Scientific Assessment of Ozone Depletion: 2010, edited by: Ennis, C. A., World Meteorological Organization Global Ozone Research and Monitoring Project - Report No. 52, 76 pp., 2011.

Druitt, T.: Emplacement of the 18 May 1980 lateral blast deposit ENE of Mount St. Helens, Washington, Bull. Volcanol., 54, 554-572, 10.1007/BF00569940, 1992.

Duncan, B. N., Logan, J. A., Bey, I., Megretskaia, I. A., Yantosca, R. M., Novelli, P. C., Jones, N. B., and Rinsland, C. P.: Global budget of CO, 1988–1997: Source estimates and validation with a global model, J. Geophys. Res., 112, D22301, 10.1029/2007jd008459, 2007.

Einstein, A.: Über einen die Erzeugung und Verwandlung des Lichtes betreffenden heuristischen Gesichtspunkt, Ann. Phys., 322, 132-148, 10.1002/andp.19053220607, in English at en.wikisource.org/wiki/A_Heuristic_Model_of_the_Creation_and_Transformation_of_Light, 1905a.

Einstein, A.: Zur elektrodynamik bewegter körper, Ann. Phys., 322, 891-921, 10.1002/andp.19053221004, in English at www.fourmilab.ch/etexts/einstein/specrel/www/, 1905b.

Environment Canada: Archive of world ozone maps: exp-studies.tor.ec.gc.ca/clf2/e/ozoneworld.html, 2013a.

Environment Canada: National climate data and information archive: www.climate.weatheroffice.gc.ca/climateData/dailydata_e.html?StationID=5097, 2013b.

EPA: Air emission sources: www.epa.gov/air/emissions/, 2012.

EPA: Air trends: www.epa.gov/air/airtrends/sulfur.html, 2013.

Etheridge, D. M., Steele, L. P., Francey, R. J., and Langenfelds, R. L.: Atmospheric methane between 1000 A.D. and present: Evidence of anthropogenic emissions and climatic variability J. Geophys. Res., 103, 15979-15993, 10.1029/98JD00923, 1998.

Fedorov, A. V., Brierley, C. M., Lawrence, K. T., Liu, Z., Dekens, P. S., and Ravelo, A. C.: Patterns and mechanisms of early Pliocene warmth, Nature, 496, 43-49, 10.1038/nature12003, 2013.

Fiedler, V., Nau, R., Ludmann, S., Arnold, F., Schlager, H., and Stohl, A.: East Asian SO_2 pollution plume over Europe–Part 1: Airborne trace gas measurements and source identification by particle dispersion model simulations, Atmos. Chem. Phys., 9, 4717–4728, 10.5194/acp-9-4717-2009, 2009.

Finlayson-Pitts, B. J., and Pitts, J. N.: Chemistry of the Upper and Lower Atmosphere: Theory, Experiments, and Applications, Academic Press, San Diego, 969 pp., 1999.

Fioletov, V.: Ozone climatology, trends, and substances that control ozone, Atmos. Ocean, 46, 39-67, 10.3137/ao.460103, 2008.

Fischer, H., Wahlen, M., Smith, J., Mastroianni, D., and Deck, B.: Ice core records of atmospheric CO_2 around the last three Glacial terminations, Science, 283, 1712-1714, 10.1126/science.283.5408.1712, 1999.

Fisher, D., Zheng, J., Burgess, D., Zdanowicz, C., Kinnard, C., Sharp, M., and Bourgeois, J.: Recent melt rates of Canadian arctic ice caps are the highest in four millennia, Global Planet. Change, 84, 3-7, 10.1016/j.gloplacha.2011.06.005, 2012.

Folland, C. K., Karl, T. R., Christy, J. R., Clarke, R. A., Gruza, G. V., Jouzel, J., Mann, M. E., Oerlemans, J., Salinger, M. J., and Wang, S.-W.: Observed climate variability and change, in: Climate Change 2001: The Scientific Basis. Contribution of Working Group I to the Third Assessment Report of the Intergovernmental Panel on Climate Change, edited by: Houghton, J. T., Ding, Y., Griggs, D. J., M. Noguer, P.J. van der Linden, Dai, X., Maskell, K., and Johnson, C. A., Cambridge University Press, 99-181, 2001.

Freda, C., Baker, D., and Scarlato, P.: Sulfur diffusion in basaltic melts, Geochim. Cosmochim. Acta, 69, 5061-5069, 10.1016/j.gca.2005.02.002, 2005.

Fröhlich, C., and Lean, J.: The sun's total irradiance: Cycles, trends and related climate change uncertainties since 1976, Geophys. Res. Lett., 25 4377-4380, 10.1029/1998GL900157, 1998.

Gardner, A. S., Moholdt, G., Wouters, B., Wolken, G. J., Burgess, D. O., Sharp, M. J., Cogley, J. G., Braun, C., and Labine, C.: Sharply increased mass loss from glaciers and ice caps in the Canadian Arctic Archipelago, Nature, 473, 357-360, 10.1038/nature10089, 2011.

Gerlach, T. M., Westrich, H. R., and Symonds, R. B.: Preeruption vapor in magma of the climactic Mount Pinatubo eruption: Source of the giant stratospheric sulfur dioxide cloud, in: Fire and mud: Eruptions and lahars of Mount Pinatubo, Philippines, edited by: Newhall, C. G., and Punongbayan, R. S., Philippine Institute of Volcanology and Seismology and University of Washington Press, 415-433, 1996.

Gleason, J., Bhartia, P. K., Herman, J. R., McPeters, R., Newman, P., Stolarski, R., Flynn, L., Labow, G., Larko, D., and Seftor, C.: Record low global ozone in 1992, Science, 260, 523, 10.1126/science.260.5107.523, 1993.

Gleckler, P. J., AchutaRao, K., Gregory, J. M., Santer, B. D., Taylor, K. E., and Wigley, T. M. L.: Krakatoa lives: The effect of volcanic eruptions on ocean heat

content and thermal expansion, Geophys. Res. Lett., 33, L17702, 10.1029/2006gl026771, 2006a.

Gleckler, P. J., Wigley, T. M. L., Santer, B. D., Gregory, J. M., AchutaRao, K., and Taylor, K. E.: Krakatoa's signature persists in the ocean, Nature, 439, 675, 10.1038/439675a, 2006b.

Global Volcanism Program: Large Holocene eruptions: www.volcano.si.edu/world/largeeruptions.cfm, 2013.

Gregory, J. M., Lowe, J. A., and Tett, S. F. B.: Simulated global-mean sea level changes over the last half-millennium, J. Clim., 19, 4576-4591, 10.1175/JCLI3881.1, 2006.

Gueymard, C.: The sun's total and spectral irradiance for solar energy applications and solar radiation models, Solar Energy, 76, 423-453, 10.1016/j.solener.2003.08.039, 2004.

HadCRUT3nh: HadCRUT3 northen hemispahere: www.cru.uea.ac.uk/cru/data/temperature/hadcrut3nh.txt, 2013.

Hadley Centre: HadAT: globally gridded radiosonde temperature anomalies from 1958 to present: www.metoffice.gov.uk/hadobs/hadat/images.html, 2013.

Haigh, J. D., Winning, A. R., Toumi, R., and Harder, J. W.: An influence of solar spectral variations on radiative forcing of climate, Nature, 467, 696-699, 10.1038/nature09426, 2010.

Hansen, G., and Chipperfield, M. P.: Ozone depletion at the edge of the Arctic polar vortex 1996/1997, J. Geophys. Res., 104, 1837-1845, 10.1029/1998JD100021, 1999.

Hansen, J., Russell, G., Lacis, A., Fung, I., Rind, D., and Stone, P.: Climate response times: dependence on climate sensitivity and ocean mixing, Science, 229, 857-859, 10.1126/science.229.4716.857, 1985.

Hansen, J., Nazarenko, L., Ruedy, R., Sato, M., Willis, J., Del Genio, A., Koch, D., Lacis, A., Lo, K., and Menon, S.: Earth's energy imbalance: Confirmation and implications, Science, 308, 1431-1435, 10.1126/science.1110252, 2005.

Hansen, J., Ruedy, R., Sato, M., and Lo, K.: Global surface temperature change, Rev. Geophys., 48, RG4004, 10.1029/2010RG000345, 2010.

Harder, J. W., Fontenla, J. M., Pilewskie, P., Richard, E. C., and Woods, T. N.: Trends in solar spectral irradiance variability in the visible and infrared, Geophys. Res. Lett., 36, L07801, 10.1029/2008gl036797, 2009.

Hassler, B., Bodeker, G., Solomon, S., and Young, P.: Changes in the polar vortex: Effects on Antarctic total ozone observations at various stations, Geophys. Res. Lett., 38, L01805, 10.1029/2010GL045542, 2011.

Herman, J. R.: Global increase in UV irradiance during the past 30 years (1979–2008) estimated from satellite data, J. Geophys. Res, 115, D04203, 10.1029/2009JD012219, 2010.

Hermans, C., Vandaele, A. C., and Fally, S.: Fourier transform measurements of SO_2 absorption cross sections: I. Temperature dependence in the 24000–29000 cm^{-1}

(345–420 nm) region, J. Quant. Spectrosc. Radiat. Transfer, 110, 756-765, 10.1016/j.jqsrt.2009.01.031, 2009.

Herweijer, C., Seager, R., Cook, E. R., and Emile-Geay, J.: North American droughts of the last millennium from a gridded network of tree-ring data, J. Clim., 20, 1353-1376, 10.1175/JCLI4042.1, 2007.

Hjartarson, Á.: Víðáttumestu hraun Íslands. (The largest lavas of Iceland), Náttúrufræðingurinn, 81, 37-49, www.hin.is/resultpage.asp?ID=2775, 2011.

Hughes, G. L., Rao, S. S., and Rao, T. S.: Statistical analysis and time-series models for minimum/maximum temperatures in the Antarctic Peninsula, Proc. Roy. Soc. London, Ser. A, 463, 241-259, 10.1098/rspa.2006.1766, 2007.

Huybers, P., and Langmuir, C.: Feedback between deglaciation, volcanism, and atmospheric CO2, Earth Planet. Sci. Lett., 286, 479-491, 10.1016/j.epsl.2009.07.014, 2009.

Hydutsky, D., Bianco, N., and Castlemanjr, A.: The photodissociation of SO_2 between 200 and 197 nm, Chem. Phys., 350, 212-219, 10.1016/j.chemphys.2008.03.001, 2008.

Jeffries, M. O., and Richter-Menge, J. A.: State of Climate in 2011 Chapter 5. The Arctic, Bull. Am. Meteorol. Soc., 93, S127-S147, www.ncdc.noaa.gov/bams-state-of-the-climate/2011.php, 2012.

Joachimski, M. M., Lai, X., Shen, S., Jiang, H., Luo, G., Chen, B., Chen, J., and Sun, Y.: Climate warming in the latest Permian and the Permian–Triassic mass extinction, Geology, 40, 195-198, 10.1130/G32707.1, 2012.

Johnston, H. S.: Expected short-term local effect of nuclear bombs on stratospheric ozone, J. Geophys. Res., 82, 3119-3124, 10.1029/JC082i021p03119, 1977.

Johnston, P., McKenzie, R., Keys, J., and Matthews, W.: Observations of depleted stratospheric NO_2 following the Pinatubo volcanic eruption, Geophys. Res. Lett., 19, 211-213, 10.1029/92GL00043, 1992.

Jones, G. S., Gregory, J. M., Stott, P. A., Tett, S. F., and Thorpe, R. B.: An AOGCM simulation of the climate response to a volcanic super-eruption, Clim. Dyn., 25, 725-738, 10.1007/s00382-005-0066-8, 2005.

Kai, F. M., Tyler, S. C., Randerson, J. T., and Blake, D. R.: Reduced methane growth rate explained by decreased Northern Hemisphere microbial sources, Nature, 476, 194-197, 10.1038/nature10259, 2011.

Karl, T., Gleason, B., Menne, M., McMahon, J., Heim Jr, R., Brewer, M., Kunkel, K., Arndt, D., Privette, J., and Bates, J.: US temperature and drought: Recent anomalies and trends, EOS Trans. Am. Geophys. Un., 93, 473, 10.1029/2012EO470001, 2012.

Keller, T.: Direct effects of sulphur dioxide on trees, Phil. Trans. R. Soc. London, Ser. B, 305, 317-325, 10.1098/rstb.1984.0060, 1984.

Kerr, J., Wardle, D., and Tarasick, D.: Record low ozone values over Canada in early 1993, Geophys. Res. Lett., 20, 1979-1982, 10.1029/93GL01927, 1993.

Kerr, R. A.: Ozone takes a nose dive after the eruption of Mt. Pinatubo, Science, 260, 490-491, 10.1126/science.260.5107.490, 1993.

Kerr, R. A.: Forecasting regional climate change flunks its first test, Science, 339, 638-638, 10.1126/science.339.6120.638 2013.

Kington, J.: The Weather of the 1780s Over Europe, Cambridge University Press, 180 pp., 2009.

Kinnison, D., Brasseur, G., Walters, S., Garcia, R., Marsh, D., Sassi, F., Harvey, V., Randall, C., Emmons, L., and Lamarque, J.: Sensitivity of chemical tracers to meteorological parameters in the MOZART-3 chemical transport model, J. Geophys. Res, 112, D20302, 10.1029/2006JD007879, 2007.

Klimont, Z., Smith, S. J., and Cofala, J.: The last decade of global anthropogenic sulfur dioxide: 2000–2011 emissions, Environ. Res. Lett., 8, 014003, 10.1088/1748-9326/8/1/014003, 2013.

Knight, J., Kennedy, J., Folland, C., Harris, G., Jones, G., Palmer, M., Parker, D., Scaife, A., and Stott, P.: Do global temperature trends over the last decade falsify climate predictions?, in: State of the Climate in 2008, edited by: Peterson, T. C., and Baringer, M. O., Bull. Am. Meteorol. Soc., 90 (8), S22-S23, 10.1175/BAMS-90-8-StateoftheClimate, 2009.

Kump, L. R., Pavlov, A., and Arthur, M. A.: Massive release of hydrogen sulfide to the surface ocean and atmosphere during intervals of oceanic anoxia, Geology, 33, 397-400, 10.1130/g21295.1, 2005.

Kump, L. R., and Barley, M. E.: Increased subaerial volcanism and the rise of atmospheric oxygen 2.5 billion years ago, Nature, 448, 1033-1036, 10.1038/nature06058, 2007.

Kutterolf, S., Jegen, M., Mitrovica, J. X., Kwasnitschka, T., Freundt, A., and Huybers, P. J.: A detection of Milankovitch frequencies in global volcanic activity, Geology, 41, 227-230, 10.1130/G33419.1, 2012.

Kwok, R., and Untersteiner, N.: The thinning of Arctic sea ice, Physics Today, 64, 36-41, 10.1063/1.3580491, 2011.

Labitzke, K., and McCormick, M.: Stratospheric temperature increases due to Pinatubo aerosols, Geophys. Res. Lett., 19, 207-210, 10.1029/91GL02940, 1992.

Laj, P., Sigurdsson, H., Drummey, S. M., Spencer, M. J., and Palais, J. M.: Depletion of H_2O_2 in a Greenland ice core: Implications for oxidation of volcanic SO_2, Nature, 346, 45-48, 10.1038/346045a0, 1990.

Lanphere, M. A., Champion, D. E., Christiansen, R. L., Izett, G. A., and Obradovich, J. D.: Revised ages for tuffs of the Yellowstone Plateau volcanic field: Assignment of the Huckleberry Ridge Tuff to a new geomagnetic polarity event, Geol. Soc. Am. Bull., 114, 559-568, 10.1130/0016-7606(2002)114, 2002.

LaRiviere, J. P., Ravelo, A. C., Crimmins, A., Dekens, P. S., Ford, H. L., Lyle, M., and Wara, M. W.: Late Miocene decoupling of oceanic warmth and atmospheric carbon dioxide forcing, Nature, 486, 97-100, 10.1038/nature11200, 2012.

Lea, D. W.: Climate Impact of Late Quaternary Equatorial Pacific Sea Surface Temperature Variations, Science, 289, 1719-1724, 10.1126/science.289.5485.1719, 2000.

Lee, C. T. A., Luffi, P., Plank, T., Dalton, H., and Leeman, W. P.: Constraints on the depths and temperatures of basaltic magma generation on Earth and other terrestrial planets using new thermobarometers for mafic magmas, Earth Planet. Sci. Lett., 279, 20-33, 10.1016/j.epsl.2008.12.020, 2009.

Lemke, P., Ren, J., Alley, R. B., Allison, I., Carrasco, J., Flato, G., Fujii, Y., Kaser, G., Mote, P., Thomas, R. H., and Zhang, T.: Observations: Changes in snow, ice, and frozen ground, in: Climate Change 2007: The physical science basis, edited by: Solomon, S., Qin, D., Manning, M., Marquis, M., Averyt, K., Tignor, M., Miller Jr, H., and Chen, Z., Cambridge University Press, 337-383, 2007.

Levitus, S., Antonov, J., Boyer, T., Baranova, O., Garcia, H., Locarnini, R., Mishonov, A., Reagan, J., Seidov, D., and Yarosh, E.: World ocean heat content and thermosteric sea level change (0-2000 m), 1955-2010, Geophys. Res. Lett., 39, L10603, 10.1029/2012GL051106, 2012.

Lewis, G. N.: The conservation of photons, Nature, 118, 874-875, 10.1038/118874a0, 1926.

Licciardi, J. M., Kurz, M. D., and Curtice, J. M.: Glacial and volcanic history of Icelandic table mountains from cosmogenic ^{3}He exposure ages, Quat. Sci. Rev., 26, 1529-1546, 10.1016/j.quascirev.2007.02.016, 2007.

Lüthi, D., Le Floch, M., Bereiter, B., Blunier, T., Barnola, J.-M., Siegenthaler, U., Raynaud, D., Jouzel, J., Fischer, H., and Kawamura, K.: High-resolution carbon dioxide concentration record 650,000–800,000 years before present, Nature, 453, 379-382, 10.1038/nature06949, 2008.

Madronich, S.: Trends and predictions in global UV, in: The Role of the Stratosphere in Global Change, edited by: Chanin, M. L., Springer-Verlag, Berlin, 463-471, 1993.

Maeder, J.: Total yearly ozone at Arosa: ftp://iaclin2.ethz.ch/pub_read/maeder/totozone_arosa_yearly, 2013.

Manley, G.: Central England temperatures: monthly means 1659 to 1973, Q. J. Roy. Meteorol. Soc., 100, 389-405, 10.1002/qj.49710042511, 1974.

Manney, G. L., Santee, M. L., Rex, M., Livesey, N. J., Pitts, M. C., Veefkind, P., Nash, E. R., Wohltmann, I., Lehmann, R., and Froidevaux, L.: Unprecedented Arctic ozone loss in 2011, Nature, 478, 469-475, 10.1038/nature10556, 2011.

Manninen, S., and Huttunen, S.: Response of needle sulphur and nitrogen concentrations of Scots pine versus Norway spruce to SO_2 and NO_2, Environ. Pollut., 107, 421-436, 10.1016/S0269-7491(99)00158-X, 2000.

Maxwell, J. C.: A treatise on electricity and magnetism, Clarendon Press, Oxford, 1873.

Mayewski, P. A., Meeker, L. D., Twickler, M. S., Whitlow, S., Yang, Q., Lyons, W. B., and Prentice, M.: Major features and forcing of high-latitude northern hemisphere atmospheric circulation using a 110,000-year-long glaciochemical series, J. Geophys. Res., 102, 26345–26366, 10.1029/96JC03365, 1997.

McBean, G., Alekseev, G., Chen, D., Førland, E., Fyfe, J., Groisman, P. Y., King, R., Melling, H., Russell Vose, and H.Whitfield, P.: Arctic Climate: Past and Present, in: Impacts of a Warming Arctic: Arctic Climate Impact Assessment, edited by: Hassol, S. J., Cambridge University Press, 2004.

McBirney, A. R.: Igneous Petrology, 3rd ed., Jones and Bartlett, Boston, 550 pp., 2007.

McCormick, M. P., and Veiga, R. E.: SAGE II measurements of early Pinatubo aerosols, Geophys. Res. Lett., 19, 155–158, 10.1029/91GL02790, 1992.

Meese, D. A., Gow, A., Grootes, P., Mayewski, P., Ram, M., Stuiver, M., Taylor, K., Waddington, E., and Zielinski, G.: The accumulation record from the GISP2 core as an indicator of climate-change throughout the Holocene, Science, 266, 1680-1682, 10.1126/science.266.5191.1680, 1994.

Meredith, M. P., and King, J. C.: Rapid climate change in the ocean west of the Antarctic Peninsula during the second half of the 20th century, Geophys. Res. Lett, 32, L19604, 10.1029/2005GL024042, 2005.

Minnis, P., Harrison, E. F., Stowe, L. L., Gibson, G. G., Denn, F. M., Doelling, D. R., and Smith, W. L., Jr.: Radiative climate forcing by the Mount Pinatubo eruption, Science, 259, 1411-1415, 10.1126/science.259.5100.1411, 1993.

Molina, M. J., and Rowland, F. S.: Stratospheric sink for chlorofluoromethanes: Chlorine catalysed destruction of ozone, Nature, 249, 810-814, 10.1038/249810a0, 1974.

Monnin, E., Indermuhle, A., Dallenbach, A., Fluckiger, J., Stauffer, B., Stocker, T. F., Raynaud, D., and Barnola, J. M.: Atmospheric CO_2 concentrations over the last glacial termination, Science, 291, 112-114, 10.1126/science.291.5501.112, 2001.

Mulvaney, R., Abram, N. J., Hindmarsh, R. C. A., Arrowsmith, C., Fleet, L., Triest, J., Sime, L. C., Alemany, O., and Foord, S.: Recent Antarctic Peninsula warming relative to Holocene climate and ice-shelf history, Nature, 489, 141-144, 10.1038/nature11391, 2012.

NASA: Ozone hole watch annual records: ozonewatch.gsfc.nasa.gov/meteorology/annual_data.html, 2013a.

NASA: Sunspot number per month: solarscience.msfc.nasa.gov/greenwch/spot_num.txt, 2013b.

Neely, R. R., Toon, O. B., Solomon, S., Vernier, J. P., Alvarez, C., English, J. M., Rosenlof, K. H., Mills, M. J., Bardeen, C. G., and Daniel, J. S.: Recent anthropogenic increases in SO_2 from Asia have minimal impact on stratospheric aerosol, Geophys. Res. Lett., 40, 999-1004, 10.1002/grl.50263, 2013.

Nemani, R., Keeling, C., Hashimoto, H., Jolly, W., Piper, S., Tucker, C., Myneni, R., and Running, S.: Climate-driven increases in global terrestrial net primary production from 1982 to 1999, Science, 300, 1560-1563, 10.1126/science.1082750, 2003.

Newhall, C. G., and Self, S.: The volcanic explosivity index (VEI) - An estimate of explosive magnitude for historical volcanism, J. Geophys. Res., 87, 1231-1238, 10.1029/JC087iC02p01231, 1982.

Nghiem, S., Hall, D., Mote, T., Tedesco, M., Albert, M., Keegan, K., Shuman, C., DiGirolamo, N., and Neumann, G.: The extreme melt across the Greenland ice sheet in 2012, Geophys. Res. Lett., 39, L20502, 10.1029/2012GL053611, 2012.

NOAA: U.S. Records: www.ncdc.noaa.gov/extremes/records/daily/maxt/2012/03/00?sts[]=US, 2012a.

NOAA: Sea Surface Temperatures Reach Record Highs on Northeast Continental Shelf: www.nefsc.noaa.gov/press_release/2012/SciSpot/SS1209/, 2012b.

NOAA: Multivariate ENSO index (MEI): www.esrl.noaa.gov/psd/enso/mei/, 2013a.

NOAA: Annual mean CO_2 at Mauna Loa: ftp.cmdl.noaa.gov/ccg/co2/trends/co2_annmean_mlo.txt 2013b.

Novakov, T.: Large historical changes of fossil-fuel black carbon aerosols, Geophys. Res. Lett., 30, 1324, 10.1029/2002gl016345, 2003.

NSIDC: Arctic sea ice reaches lowest extent for the year and the satellite record: nsidc.org/news/press/2012_seaiceminimum.html, 2012.

Palais, J., and Sigurdsson, H.: Petrologic evidence of volatile emissions from major historic and pre-historic volcanic eruptions, in Understanding Climate Change, Geophys. Monogr., 52, 31-56, 10.1029/GM052p0031, 1989.

PALEOSENS Project Members: Making sense of palaeoclimate sensitivity, Nature, 491, 683-691, 10.1038/nature11574, 2012.

Parker, D., Legg, T., and Folland, C.: A new daily central England temperature series, 1772–1991, Int. J. Climatol., 12, 317–342, 10.1002/joc.3370120402, 1992.

Parkinson, C. L., and Cavalieri, D. J.: Antarctic sea ice variability and trends, 1979-2010, The Cryosphere, 6, 871-880, 10.5194/tc-6-871-2012, 2012.

Parrenin, F., Masson-Delmotte, V., Köhler, P., Raynaud, D., Paillard, D., Schwander, J., Barbante, C., Landais, A., Wegner, A., and Jouzel, J.: Synchronous change of atmospheric CO_2 and Antarctic temperature during the last deglacial warming, Science, 339, 1060-1063, 10.1126/science.1226368, 2013.

Pedro, J. B., Rasmussen, S. O., and van Ommen, T. D.: Tightened constraints on the time-lag between Antarctic temperature and CO_2 during the last deglaciation, Clim. Past, 8, 1213-1221, 10.5194/cp-8-1213-2012, 2012.

Petit, J. R., Jouzel, J., Raynaud, D., Barkov, N. I., Barnola, J.-M., Basile, I., Bender, M., Chappellaz, J., Davis, M., Delaygue, G., Delmotte, M., Kotlyakov, V. M., Legrand, M., Lipenkov, V. Y., Lorius, C., Pepin, L., Ritz, C., Saltzman, E., and Stievenard, M.: Climate and atmospheric history of the past 420,000 years from the Vostok ice core, Antarctica, Nature, 399, 429-436, 10.1038/20859, 1999.

Planck, M.: Entropie und temperatur strahlender wärme, Ann. Phys., 306, 719-737, 10.1002/andp.19003060410, 1900.

Planck, M.: Ueber das gesetz der energieverteilung im normalspectrum (On the law of distribution of energy in the normal spectrum), Ann. Phys., 309, 3, 553-560, 10.1002/andp.19013090310, 1901.

Polvani, L. M., Waugh, D. W., Correa, G. J. P., and Son, S. W.: Stratospheric ozone depletion: The main driver of twentieth-century atmospheric circulation changes in the Southern Hemisphere, J. Clim., 24, 795-812, 10.1175/2010JCLI3772.1, 2011.

Purkey, S. G., and Johnson, G. C.: Global contraction of Antarctic bottom water between the 1980s and 2000s, J. Clim., 25, 5830-5844, 10.1175/JCLI-D-11-00612.1, 2012.

Rahmstorf, S.: Timing of abrupt climate change: A precise clock, Geophys. Res. Lett., 30, 1510, 10.1029/2003gl017115, 2003.

Randel, W. J., Wu, F., Vömel, H., Nedoluha, G. E., and Forster, P.: Decreases in stratospheric water vapor after 2001: Links to changes in the tropical tropopause and the Brewer-Dobson circulation, J. Geophys. Res., 111, D12312, 10.1029/2005jd006744, 2006.

Randel, W. J.: Variability and trends in stratospheric temperature and water vapor, in The Stratosphere: Dynamics, Transport and Chemistry, Geophys. Monogr., 190, 123-135, 10.1029/2009GM000870, 2010.

Rashid, H., Polyak, L., and Mosley-Thompson, E.: Abrupt climate change revisited, Geophys. Monogr., 193, 1-14, 10.1029/2011GM001139, 2011.

Rayner, N., Brohan, P., Parker, D., Folland, C., Kennedy, J., Vanicek, M., Ansell, T., and Tett, S.: Improved analyses of changes and uncertainties in sea surface temperature measured in situ since the mid-nineteenth century: the HadSST2 dataset, J. Clim., 19, 446-469, 10.1175/JCLI3637.1, 2006.

Reed, R. J.: The role of vertical motion in ozone-weather relationship, J. Meteorol., 7, 263-267, 10.1175/1520-0469(1950)007<0263:TROVMI>2.0.CO;2, 1950.

Reichow, M. K., Pringle, M., Al'Mukhamedov, A., Allen, M., Andreichev, V., Buslov, M., Davies, C., Fedoseev, G., Fitton, J., and Inger, S.: The timing and extent of the eruption of the Siberian Traps large igneous province: Implications for the end-Permian environmental crisis, Earth Planet. Sci. Lett., 277, 9-20, 10.1016/j.epsl.2008.09.030, 2009.

Remote Sensing Systems: Description of MSU and AMSU data products: www.remss.com/msu/msu_data_description.html, 2012.

Rignot, E., Velicogna, I., van den Broeke, M. R., Monaghan, A., and Lenaerts, J.: Acceleration of the contribution of the Greenland and Antarctic ice sheets to sea level rise, Geophys. Res. Lett., 38, L05503, 10.1029/2011gl046583, 2011.

Robock, A.: Volcanic eruptions and climate, Rev. Geophys., 38, 191-219, 10.1029/1998RG000054, 2000.

Robock, A.: Pinatubo eruption: The climatic aftermath, Science, 295, 1242-1244, 10.1126/science.1069903, 2002.

Rohde, R. A.: Radiation transmitted by the atmosphere: commons.wikimedia.org/wiki/File:Atmospheric_Transmission.png, 2013.

Röhl, U., Bralower, T. J., Norris, R. D., and Wefer, G.: New chronology for the late Paleocene thermal maximum and its environmental implications, Geology, 28, 927-930, 10.1130/0091-7613(2000)28<927:ncftlp>2.0.co;2, 2000.

Rohrer, F., and Berresheim, H.: Strong correlation between levels of tropospheric hydroxyl radicals and solar ultraviolet radiation, Nature, 442, 184-187, 10.1038/nature04924, 2006.

Rothman, L. S., Gordon, I. E., Barbe, A., Benner, D. C., Bernath, P. F., Birk, M., Boudon, V., Brown, L. R., Campargue, A., and Champion, J. P.: The HITRAN 2008 molecular spectroscopic database, J. Quant. Spectrosc. Radiat. Transfer, 110, 533-572, 10.1016/j.jqsrt.2009.02.013, 2009.

Royer, D.: CO_2-forced climate thresholds during the Phanerozoic, Geochim. Cosmochim. Acta, 70, 5665-5675, 10.1016/j.gca.2005.11.031, 2006.

Sallenger Jr, A. H., Doran, K. S., and Howd, P. A.: Hotspot of accelerated sea-level rise on the Atlantic coast of North America, Nature Clim. Change, 2, 884-888, 10.1038/NCLIMATE1597, 2012.

Schultz, M., and Rast, S.: REanalysis of the TROpospheric chemical composition over the past 40 years: retro.enes.org/reports/D1-6_final.pdf 2008.

Scott, W. E., Hoblitt, R. P., Torres, R. C., Self, S., Martinez, M., and Nillos, T.: Pyroclastic flows of the 15 June, 1991, paroxysmal eruption, Mount Pinatubo, in: Fire and mud: Eruptions and lahars of Mount Pinatubo, Philippines, edited by: Newhall, C. G., and Punongbayan, R. S., Philippine Institute of Volcanology and Seismology and University of Washington Press, 545–570, 1996.

Segschneider, J., Beitsch, A., Timmreck, C., Brovkin, V., Ilyina, T., Jungclaus, J., Lorenz, S., Six, K., and Zanchettin, D.: Impact of an extremely large magnitude volcanic eruption on the global climate and carbon cycle estimated from ensemble Earth System Model simulations, Biogeosciences, 10, 669-687, 10.5194/bg-10-669-2013, 2013.

Seidel, D. J., and Randel, W. J.: Variability and trends in the global tropopause estimated from radiosonde data, J. Geophys. Res., 111, D21101, 10.1029/2006jd007363, 2006.

Seidel, D. J., Fu, Q., Randel, W. J., and Reichler, T. J.: Widening of the tropical belt in a changing climate, Nature Geosci., 1, 21-24, 10.1038/ngeo.2007.38, 2008.

Self, S., Zhao, J.-X., Holasek, R. E., Torres, R. C., and King, A. J.: The atmospheric impact of the 1991 Mount Pinatubo eruption, in: Fire and Mud: Eruptions and lahars of Mount Pinatubo, Philippines, edited by: Newhall, C. G., and Punongbayan, R. S., Philippine Institute of Volcanology and Seismology and University of Washington Press, 1089-1115, 1996.

Self, S.: The effects and consequences of very large explosive volcanic eruptions, Phil. Trans. R. Soc. London, Ser. A, 364, 2073-2097, 10.1098/rsta.2006.1814, 2006.

Self, S., Blake, S., Sharma, K., Widdowson, M., and Sephton, S.: Sulfur and chlorine in late Cretaceous Deccan magmas and eruptive gas release, Science, 319, 1654-1657, 10.1126/science.1152830, 2008.

Serreze, M. C., and Barry, R. G.: Processes and impacts of Arctic amplification: A research synthesis, Global Planet. Change, 77, 85-96, 10.1016/j.gloplacha.2011.03.004, 2011.

Severinghaus, J. P.: Abrupt climate change at the end of the last glacial period inferred from trapped air in polar ice, Science, 286, 930-934, 10.1126/science.286.5441.930, 1999.

Shakun, J. D., Clark, P. U., He, F., Marcott, S. A., Mix, A. C., Liu, Z., Otto-Bliesner, B., Schmittner, A., and Bard, E.: Global warming preceded by increasing carbon dioxide concentrations during the last deglaciation, Nature, 484, 49-54, 10.1038/nature10915, 2012.

Siebert, L., Simkin, T., and Kimberly, P.: Volcanoes of the World, 3 ed., University of California Press, Berkeley, 551 pp., 2010.

Siegenthaler, L., D., Le Floch, M., Bereiter, B., Blunier, T., Barnola, J. M., Siegenthaler, U., Raynaud, D., Jouzel, J., Fischer, H., Kawamura, K., and Stocker, T. F.: High-resolution carbon dioxide concentration record 650,000-800,000 years before present, Nature, 453, 379-382, 10.1038/nature06949, 2008.

Siegenthaler, U., Stocker, T. F., Monnin, E., Luthi, D., Schwander, J., Stauffer, B., Raynaud, D., Barnola, J. M., Fischer, H., Masson-Delmotte, V., and Jouzel, J.: Stable carbon cycle-climate relationship during the Late Pleistocene, Science, 310, 1313-1317, 10.1126/science.1120130, 2005.

Sigmundsson, F., Hreinsdóttir, S., Hooper, A., Árnadóttir, T., Pedersen, R., Roberts, M. J., Óskarsson, N., Auriac, A., Decriem, J., and Einarsson, P.: Intrusion triggering of the 2010 Eyjafjallajökull explosive eruption, Nature, 468, 426-430, 10.1038/nature09558, 2010.

Slanger, T., Jusinski, L., Black, G., and Gadd, G.: A new laboratory source of ozone and its potential atmospheric implications, Science, 241, 945-950, 10.1126/science.241.4868.945, 1988.

Sluijs, A., Schouten, S., Pagani, M., Woltering, M., Brinkhuis, H., Damste, J. S. S., Dickens, G. R., Huber, M., Reichart, G.-J., Stein, R., Matthiessen, J., Lourens, L. J., Pedentchouk, N., Backman, J., Moran, K., and the Expedition 302 Scientists: Subtropical Arctic Ocean temperatures during the Palaeocene/Eocene thermal maximum, Nature, 441, 610-613, 10.1038/nature04668, 2006.

Smith, S. J., van Aardenne, J., Klimont, Z., Andres, R. J., Volke, A., and Delgado Arias, S.: Anthropogenic sulfur dioxide emissions: 1850–2005, Atmos. Chem. Phys., 11, 1101-1116, 10.5194/acp-11-1101-2011, 2011.

Smith, T. M., Reynolds, R. W., Peterson, T. C., and Lawrimore, J.: Improvements to NOAA's historical merged land-ocean surface temperature analysis (1880-2006), J. Clim., 21, 2283-2296, 10.1175/2007JCLI2100.1, 2008.

Solomon, S.: Stratospheric ozone depletion: A review of concepts and history, Rev. Geophys., 37, 275-316, 10.1029/1999RG900008, 1999.

Solomon, S., Rosenlof, K. H., Portmann, R. W., Daniel, J. S., Davis, S. M., Sanford, T. J., and Plattner, G. K.: Contributions of stratospheric water vapor to decadal changes in the rate of global warming, Science, 327, 1219-1223, 10.1126/science.1182488, 2010.

SPARC: The Role of Halogen Chemistry in Polar Stratospheric Ozone Depletion: www.atmosp.physics.utoronto.ca/SPARC/HalogenChem_Final_20090213.pdf, 2009.

Staehelin, J., Renaud, A., Bader, J., McPeters, R., Viatte, P., Hoegger, B., Bugnion, V., Giroud, M., and Schill, H.: Total ozone series at Arosa (Switzerland): Homogenization and data comparison, J. Geophys. Res., 103, 5827-5841, 10.1029/97JD02402, 1998.

Staffelbach, T., Neftel, A., Stauffer, B., and Jacob, D.: Formaldehyde in polar ice cores: a possibility to characterize the atmospheric sink of methane in the past, Nature, 349, 603-605, 10.1038/349603a0, 1991.

Stammerjohn, S. E., Martinson, D. G., Smith, R. C., and Iannuzzi, R. A.: Sea ice in the western Antarctic Peninsula region: Spatio-temporal variability from ecological

and climate change perspectives, Deep Sea Res. II, 55, 2041-2058, 10.1016/j.dsr2.2008.04.026, 2008.

Stone, R. S., Keys, J., and Dutton, E. G.: Properties and decay of stratospheric aerosols in the Arctic following the 1991 eruptions of Mount Pinatubo, Geophys. Res. Lett., 20, 2539-2362, 10.1029/93GL02684, 1993.

Storey, M., Duncan, R., and Tegner, C.: Timing and duration of volcanism in the North Atlantic Igneous Province: Implications for geodynamics and links to the Iceland hotspot, Chem. Geol., 241, 264-281, 10.1016/j.chemgeo.2007.01.016, 2007.

Stott, L., Timmermann, A., and Thunell, R.: Southern Hemisphere and deep-sea warming led deglacial atmospheric CO_2 rise and tropical warming, Science, 318, 435-438, 10.1126/science.1143791, 2007.

Sun, Y., Joachimski, M. M., Wignall, P. B., Yan, C., Chen, Y., Jiang, H., Wang, L., and Lai, X.: Lethally Hot Temperatures During the Early Triassic Greenhouse, Science, 338, 366-370, 10.1126/science.1224126, 2012.

Svensen, H., Planke, S., Polozov, A. G., Schmidbauer, N., Corfu, F., Podladchikov, Y. Y., and Jamtveit, B.: Siberian gas venting and the end-Permian environmental crisis, Earth Planet. Sci. Lett., 277, 490-500, 10.1016/j.epsl.2008.11.015, 2009.

Tabazadeh, A., and Turco, R. P.: Stratospheric chlorine injection by volcanic eruptions: HCl scavenging and implications for ozone, Science, 260, 1082-1084, 10.1126/science.260.5111.1082, 1993.

Tachikawa, K., Vidal, L., Sonzogni, C., and Bard, E.: Glacial/interglacial sea surface temperature changes in the Southwest Pacific ocean over the past 360 ka, Quat. Sci. Rev., 28, 1160-1170, 10.1016/j.quascirev.2008.12.013, 2009.

Tedetti, M., and Sempéré, R.: Penetration of ultraviolet radiation in the marine environment. A review, Photochem. Photobiol., 82, 389-397, 10.1562/2005-11-09-IR-733, 2006.

Thompson, D. W. J., and Solomon, S.: Understanding recent stratospheric climate change, J. Clim., 22, 1934-1943, 10.1175/2008JCLI2482.1, 2009.

Thompson, D. W. J., Seidel, D. J., Randel, W. J., Zou, C. Z., Butler, A. H., Mears, C., Osso, A., Long, C., and Lin, R.: The mystery of recent stratospheric temperature trends, Nature, 491, 692-697, 10.1038/nature11579, 2012.

Thorarinsson, S.: Hekla: A notorius volcano, Almenna Bokafelagid, Reykjavik, 54 pp., 1970.

Thorarinsson, S., and Sigvaldason, G.: The Hekla eruption of 1970, Bull. Volcanol., 36, 269-288, 10.1007/BF02596870, 1972.

Thordarson, T., and Self, S.: Atmospheric and environmental effects of the 1783–1784 Laki eruption: A review and reassessment, J. Geophys. Res., 108, 4011, 10.1029/2001jd002042, 2003.

Tingley, M. P., and Huybers, P.: Recent temperature extremes at high northern latitudes unprecedented in the past 600 years, Nature, 496, 201-205, 10.1038/nature11969, 2013.

Trenberth, K., and Fasullo, J.: Tracking Earth's Energy, Science, 328, 316-317, 10.1126/science.1187272, 2010.

Trenberth, K. E., Jones, P. D., Ambenje, P., Bojariu, R., Easterling, D., Tank, A. K., Parker, D., Rahimzadeh, F., Renwick, J. A., Rusticucci, M., Soden, B., and Zhai, P.: Observations: Surface and Atmospheric Climate Change, in: Climate Change 2007: The Physical Science Basis. Contribution of Working Group I to the Fourth Assessment Report of the Intergovernmental Panel on Climate Change, edited by: Solomon, S., Qin, D., Manning, M., Chen, Z., Marquis, M., Averyt, K. B., Tignor, M., and Miller, H. L., Cambridge University Press, 235-336, 2007.

Trenberth, K. E.: An imperative for climate change planning: tracking Earth's global energy, Curr. Opin. Environ. Sustain., 1, 19-27, 10.1016/j.cosust.2009.06.001, 2009.

Trenberth, K. E., Fasullo, J. T., and Kiehl, J.: Earth's Global Energy Budget, Bull. Am. Meteorol. Soc., 90, 311-323, 10.1175/2008bams2634.1, 2009.

Trenberth, K. E., and Fasullo, J. T.: Tracking Earth’s energy: From El Niño to global warming, Surv. Geophys., 33, 413-426, 10.1007/s10712-011-9150-2, 2011.

Turco, R. P.: Photodissociation rates in the atmosphere below 100km, Surv. Geophys., 2, 153-192, 10.1007/BF01447907, 1975.

U. S. Environmental Protection Agency: National Air Pollutant Emission Trends, 1900 - 1998, www.epa.gov/ttnchie1/trends/trends98/, 238 pp., 2000.

Vance, A., McGonigle, A. J. S., Aiuppa, A., Stith, J. L., Turnbull, K., and von Glasow, R.: Ozone depletion in tropospheric volcanic plumes, Geophys. Res. Lett., 37, L22802, 10.1029/2010gl044997, 2010.

Vandaele, A. C., Hermans, C., and Fally, S.: Fourier transform measurements of SO_2 absorption cross sections: II. Temperature dependence in the 29000–44000 cm^{-1} (227–345 nm) region, J. Quant. Spectrosc. Radiat. Transfer, 110, 2115-2126, 10.1016/j.jqsrt.2009.05.006, 2009.

Vaughan, D. G., Marshall, G. J., Connolley, W. M., Parkinson, C., Mulvaney, R., Hodgson, D. A., King, J. C., Pudsey, C. J., and Turner, J.: Recent rapid regional climate warming on the Antarctic Peninsula, Clim. Change, 60, 243-274, 10.1023/A:1026021217991, 2003.

Visscher, H., Looy, C. V., Collinson, M. E., Brinkhuis, H., Van Konijnenburg-Van Cittert, J. H. A., Kürschner, W. M., and Sephton, M. A.: Environmental mutagenesis during the end-Permian ecological crisis, Proc. Nat. Acad. Sci. U.S.A., 101, 12952–12956, 2004.

von Glasow, R.: Atmospheric chemistry in volcanic plumes, Proc. Nat. Acad. Sci. U.S.A., 107, 6594-6599, 10.1073/pnas.0913164107, 2010.

Wang, X., and Zender, C. S.: Arctic and Antarctic diurnal and seasonal variations of snow albedo from multiyear Baseline Surface Radiation Network measurements, J. Geophys. Res., 116, F03008, 10.1029/2010JF001864, 2011.

Wang, Y., and Jacob, D. J.: Anthropogenic forcing on tropospheric ozone and OH since preindustrial times, J. Geophys. Res., D23, 31123-31136, 10.1029/1998JD100004, 1998.

Ward, P. L.: New interpretation of the geology of Iceland, Geol. Soc. Am. Bull., 82, 2991-3012, 10.1130/0016-7606(1971)82[2991:NIOTGO]2.0.CO;2, 1971.

Ward, P. L.: Subduction cycles under western North America during the Mesozoic and Cenozoic eras, in: Jurassic Magmatism and Tectonics of the North American Cordillera, edited by: Miller, D. M., and Busby, C., Geological Society of America Special Paper 299, 1-45, 10.1130/SPE299-p1, 1995.

Ward, P. L.: Sulfur dioxide initiates global climate change in four ways, Thin Solid Films, 517, 3188-3203, 10.1016/j.tsf.2009.01.005, 2009.

Ward, P. L.: Understanding volcanoes may be the key to controlling global warming, Soc. Vac. Coaters Bull., Summer, 26-34, 2010.

Ward, P. L.: Animation of daily northern hemisphere ozone maps 1 January 1991 to 10 May 1991: http://www.youtube.com/watch?v=5y1PU2Qu3ag, 2013a.

Ward, P. L.: Animation of daily northern hemisphere ozone maps 1 December 2009 to 30 April 2010: https://www.youtube.com/watch?v=wJFZcPEfoR4, 2013b.

Waugh, D. W., and Polvani, L. M.: Stratospheric polar vortices, in The Stratosphere: Dynamics, Transport, and Chemistry, Geophys. Monogr., 190, 43-57, 10.1029/2009GM000887, 2010.

Waugh, D. W., Primeau, F., DeVries, T., and Holzer, M.: Recent changes in the ventilation of the southern oceans, Science, 339, 568-570, 10.1126/science.1225411, 2013.

Webb, J. D., and Meaden, G. T.: Daily temperature extremes for Britain, Weather, 55, 298-315, 2012.

White, J. W. C., Barlow, L. K., Fisher, D., Grootes, P. M., Jouzel, J., Johnsen, S. J., Stuiver, M., and Clausen, H. B.: The climate signal in the stable isotopes of snow from Summit, Greenland: Results of comparisons with modern climate observations, J. Geophys. Res., 102, 26425-26439, 10.1029/97JC00162, 1997.

Wight, G., Van der Wiel, M., and Brion, C.: Dipole excitation, ionization and fragmentation of N_2 and CO in the 10-60 eV region, J. Phys. B, 9, 675-689, 10.1088/0022-3700/9/4/017, 2001.

Wignall, P.: The link between large igneous province eruptions and mass extinctions, Elements, 1, 293-297, 10.2113/gselements.1.5.293, 2005.

Wikipedia: Nuclear weapon testing: en.wikipedia.org/wiki/Nuclear_weapons_testing, 2013a.

Wikipedia: Fluorescent lamp: Phosphors and the spectrum of emitted light: en.wikipedia.org/wiki/Fluorescent_lamp#Phosphors_and_the_spectrum_of_emitted_light, 2013b.

Wild, M.: Global dimming and brightening: A review, J. Geophys. Res., 114, D00D16, 10.1029/2008jd011470, 2009.

Woods, T. N., Tobiska, W. K., Rottman, G. J., and Worden, J. R.: Improved solar Lyman a irradiance modeling from 1947 through 1999 based on UARS observations, J. Geophys. Res., 105, 27195-27215, 10.1029/2000JA000051, 2000.

WOUDC: World Ozone and Ultraviolet Radiation Data Center,: www.woudc.org/data_e.html, 2013.

Young, T.: On the nature of light and colours, Phil. Trans. R. Soc. London, 92, 12-48, www.jstor.org/stable/pdfplus/107113.pdf, 1802.

Zander, R., Demoulin, P., Ehhalt, D., Schmidt, U., and Rinsland, C.: Secular increase of the total vertical column abundance of carbon monoxide above central Europe since 1950, J. Geophys. Res., 94, 11021-11011,11028, 10.1029/JD094iD08p11021, 1989.

Zeebe, R. E., Zachos, J. C., and Dickens, G. R.: Carbon dioxide forcing alone insufficient to explain Palaeocene–Eocene Thermal Maximum warming, Nature Geosci., 2, 576-580, 10.1038/ngeo578, 2009.

Zielinski, G. A., Mayewski, P. A., Meeker, L. D., Whitlow, S., and Twickler, M.: A 110,000-year record of explosive volcanism from the GISP2 (Greenland) ice core, Quat. Res., 45, 109-118, 10.1006/qres.1996.0013, 1996.

Table 1. Comparison of explosive volcanic eruptions with extrusive volcanic eruptions. Explosive eruptions are short-lived but form aerosols in the lower stratosphere that cool Earth. Extrusive eruptions last much longer, extruding much more magma, but inject little into the stratosphere. DRE is dense-rock equivalent. Data for Pinatubo from Self et al. (1996), Scott et al. (1996), Gerlach et al. (1996), (Bureau et al., 2000) and (Robock, 2002); Laki from Thordarson and Self (2003); Yellowstone from Christiansen (2001), Lanphere et al. (2002), Jones et al. (2005) and (Segschneider et al., 2013); Siberian Traps from Reichow et al. (2009), Black et al. (2012), and Joachimski et al. (2012).

Table 1.

Explosive eruptions are short-lived but form aerosols in the lower stratosphere that cool Earth. Extrusive eruptions last much longer, extruding much more magma, but inject little into the stratosphere. DRE is dense-rock equivalent. Data for Pinatubo from Self et al. (1996), Scott et al. (1996), Gerlach et al. (1996), (Bureau et al., 2000) and (Robock, 2002); Laki from Thordarson and Self (2003); Yellowstone from Christiansen (2001), Lanphere et al. (2002), Jones et al. (2005) and (Segschneider et al., 2013); Siberian Traps from Reichow et al. (2009), Black et al. (2012), and Joachimski et al. (2012).

	An Explosive Eruption	An Extrusive Eruption	Extreme Explosive Eruption	Extreme Extrusive Eruption
Volcano	Pinatubo (1991)	Laki (1783)	Yellowstone (2.059 Ma)	Siberian Traps (250 Ma)
Primary magma type	dacite	basalt	rhyolite	basalt
Duration of longest eruptive phase	9 hours	8 days	a few hours to days	
Duration of emissions	5 days	8 months		670,000+ years
Volume of eruptives (DRE)	5 km^3			
Bulk volume of pyroclastic fallout	4 km^3	0.4 km^3		
Dominant type of mass flow	ignimbrite	basaltic lava	ignimbrite	basaltic lava
Bulk volume of mass flow	6 km^3	15 km^3	2,450 km^3	3 million km^3
Area of mass flow	400 km^2	565 km^2	15,500 km^2	5 million km^2
Caldera formed	2.5 km diameter		75 km long 45 km wide	
Eruption columns to	35 km	13 km		
SO_2 emissions	17 Mt	122 Mt		7 Gt sulphur
H_2O emissions	491-921 Mt	235 Mt		
Chlorine emissions	3-16 Mt	15 Mt		
Fluorine emissions		7 Mt		
Bromine emissions	11-25 kt			
Maximum regional SO_2 concentrations	300 ppbm	1000 ppbm		
Average effect on climate	up to -0.5°C for 3 years		up to -4°C for 6 years	+8°C warming low-latitude sea surface
Warming of lower stratosphere	+3°C within 5 months			
Peak change in surface temperature	-0.7°C	+3.3°C in NW Europe	-10°C for a few months	
Northern continental winter temperature	+3°C			

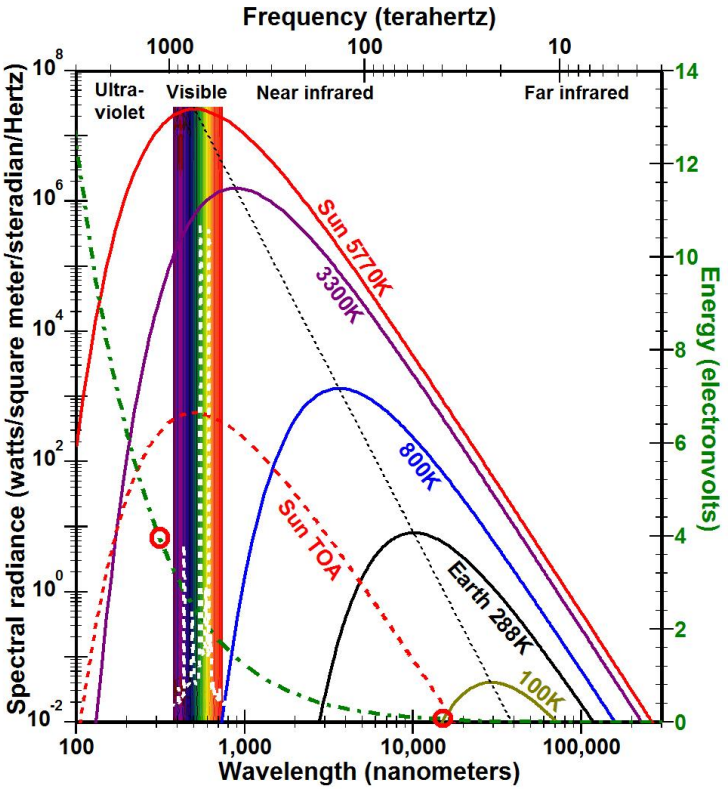

Figure 1. The spectral radiance of radiation emitted by a black body increases with the absolute temperature (K) of the body according to Planck's law. Only radiation from a black body warmer than Earth can increase the spectral amount and the frequency of peak spectral radiation (dashed black line) warming Earth. The peak spectral radiance of terrestrial radiation (black line) is 69 times less than the peak spectral radiance of solar radiation at the top of the atmosphere (Sun TOA) (red dashed line). The energy contained within radiation increases with increasing frequency (decreasing wavelength) according to Planck's postulate (E=hv) (green dot-dashed line). The infrared energy around 15,000 nm radiated by Earth and available to be absorbed by greenhouse gases is 48 times less than the solar ultraviolet energy around 310 nm absorbed by ozone or allowed to reach Earth when ozone is depleted (red circles). This factor of 48 is included within the factor of 69.

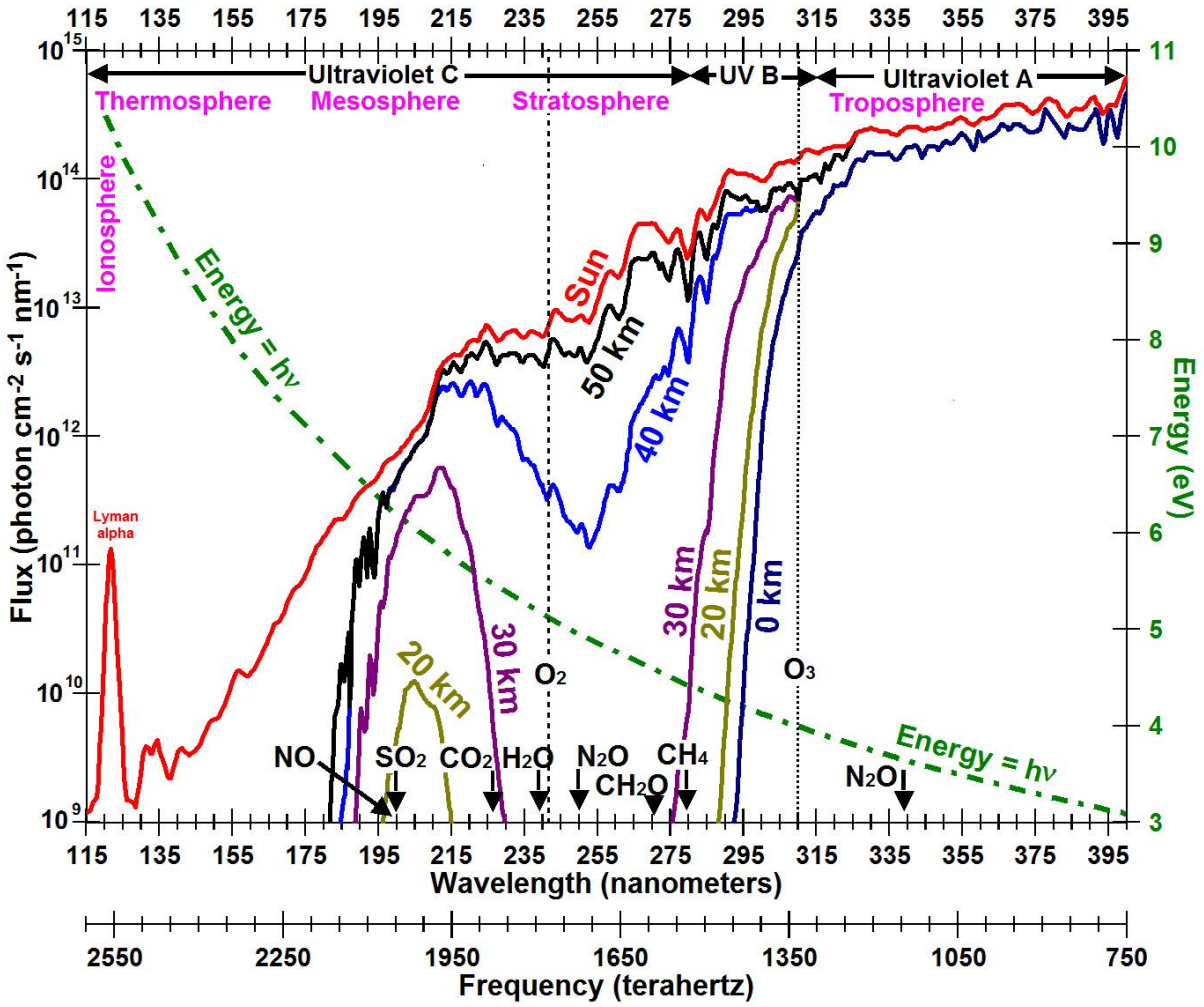

Figure 2. Nearly all ultraviolet energy from Sun (red line) at wavelengths less than 180 nm is absorbed above the stratosphere (black line at 50 km) and most at wavelengths below 290 nm is absorbed above the troposphere. Global warming occurs when energy normally absorbed in the stratosphere reaches Earth's surface.

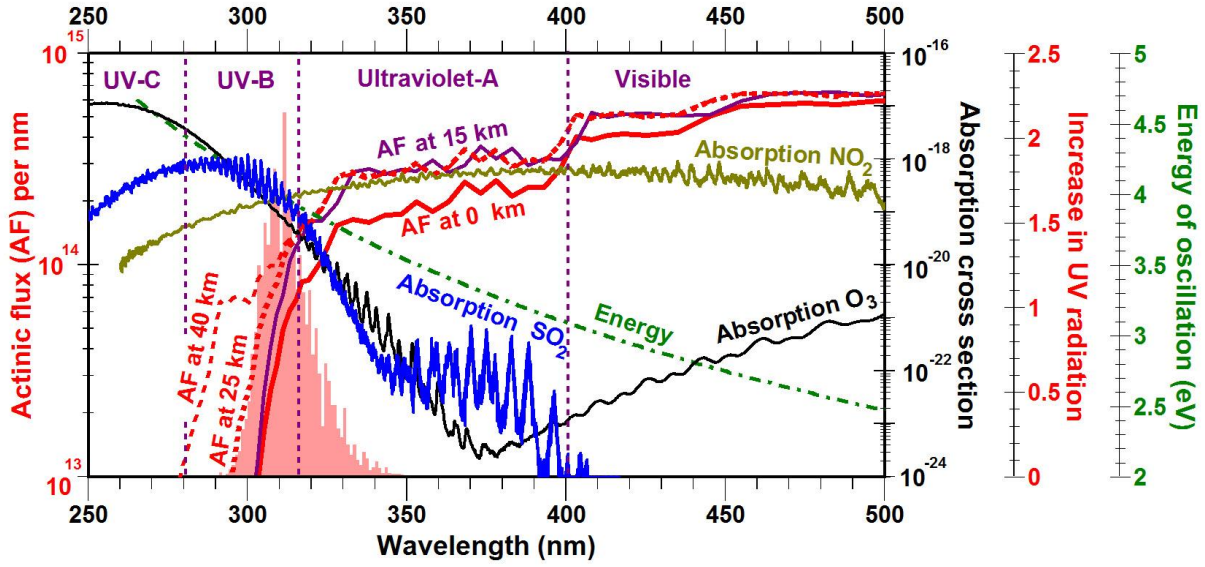

Figure 3. A 50% decrease in total column ozone increases the amount of ultraviolet radiation reaching Earth's surface by ~2 W m^{-2} between 290 and 340 nm (red shaded area) when Sun is directly overhead (Madronich, 1993). O_3, SO_2, and NO_2 absorb solar energy strongly at wavelengths <400 nm. Absorption by O_3 and NO_2 typically leads to photodissociation for wavelengths <411 nm. Actinic flux is photons cm^{-2} s^{-1}, absorption cross section is cm^2 per molecule, and increase in UV radiation is mW m^{-2} nm^{-1}. Absorption data for NO_2 and O_3 from Rothman (2009), for SO_2 from Hermans et al. (2009) and Vandaele et al. (2009).

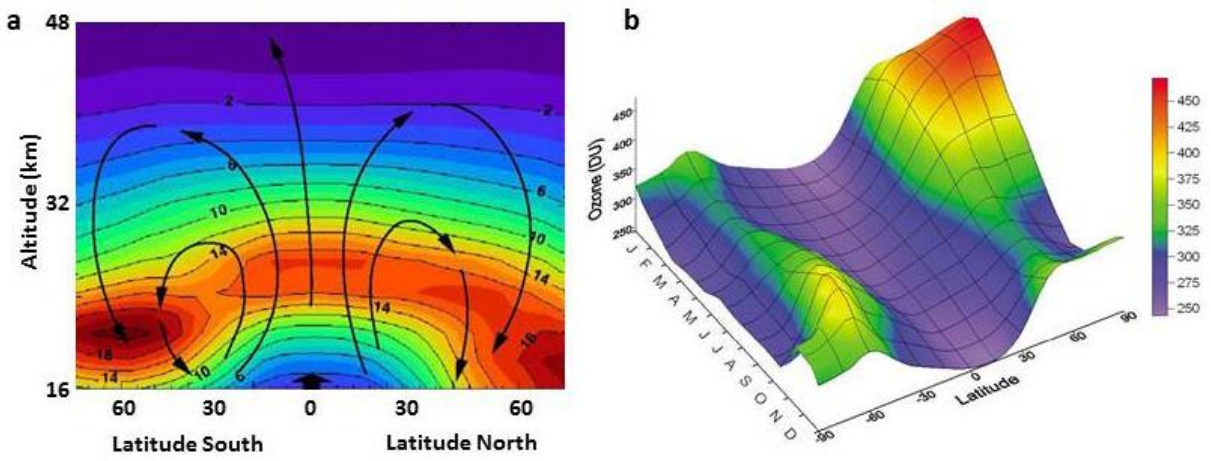

Figure 4. Ozone is created primarily in the tropics and accumulates at mid-to-polar latitudes especially in winter. a, The Brewer-Dobson Circulation observed in the winter hemisphere only via the Nimbus-7 SBUV from 1980 to 1989 in Dobson Units per kilometre copied from Cordero et al. (2003). b, A surface plot of zonal monthly mean total ozone in Dobson Units as a function of latitude and month estimated from ground-based data for the period 1964 to 1980 copied from (Fioletov, 2008).

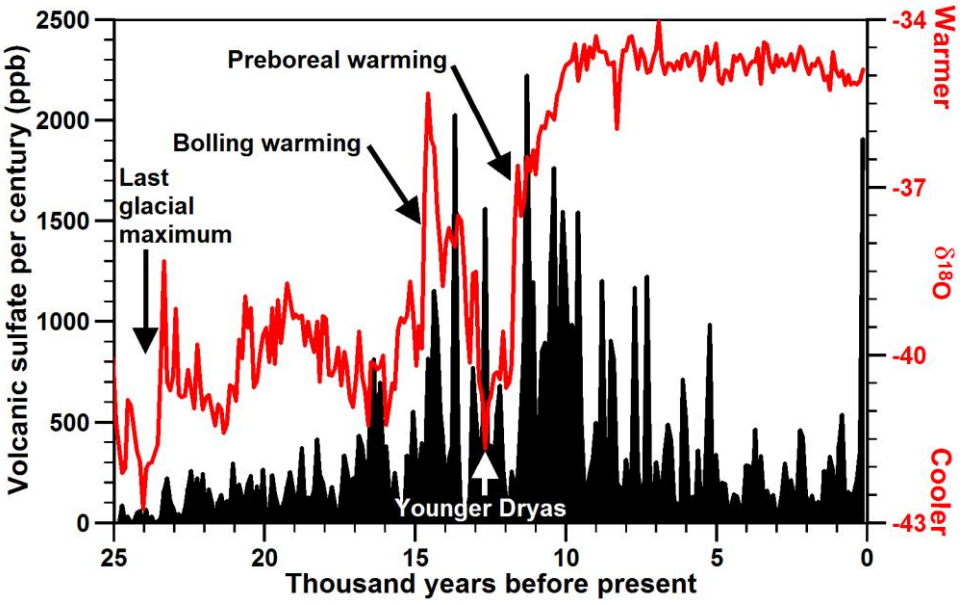

Figure 5. Volcanic sulphate per century (black) is unusually high during periods of rapid warming (red), suggesting volcanism is contemporaneous with global warming. Volcanic sulphate ranges from 0 to 2028 ppb. The increase in equatorial Pacific sea surface temperature since the last glacial maximum is on the order of 2.8^{o}C (Lea, 2000). “Volcanic” sulphate during the 20th century was caused primarily by anthropogenic emissions from northern Russia, northern Europe, and central North America (Barrie et al., 1981; Ward, 2009). The value shown (1910 ppb) is twice the sum observed during the 50 years from 1935 through 1984.

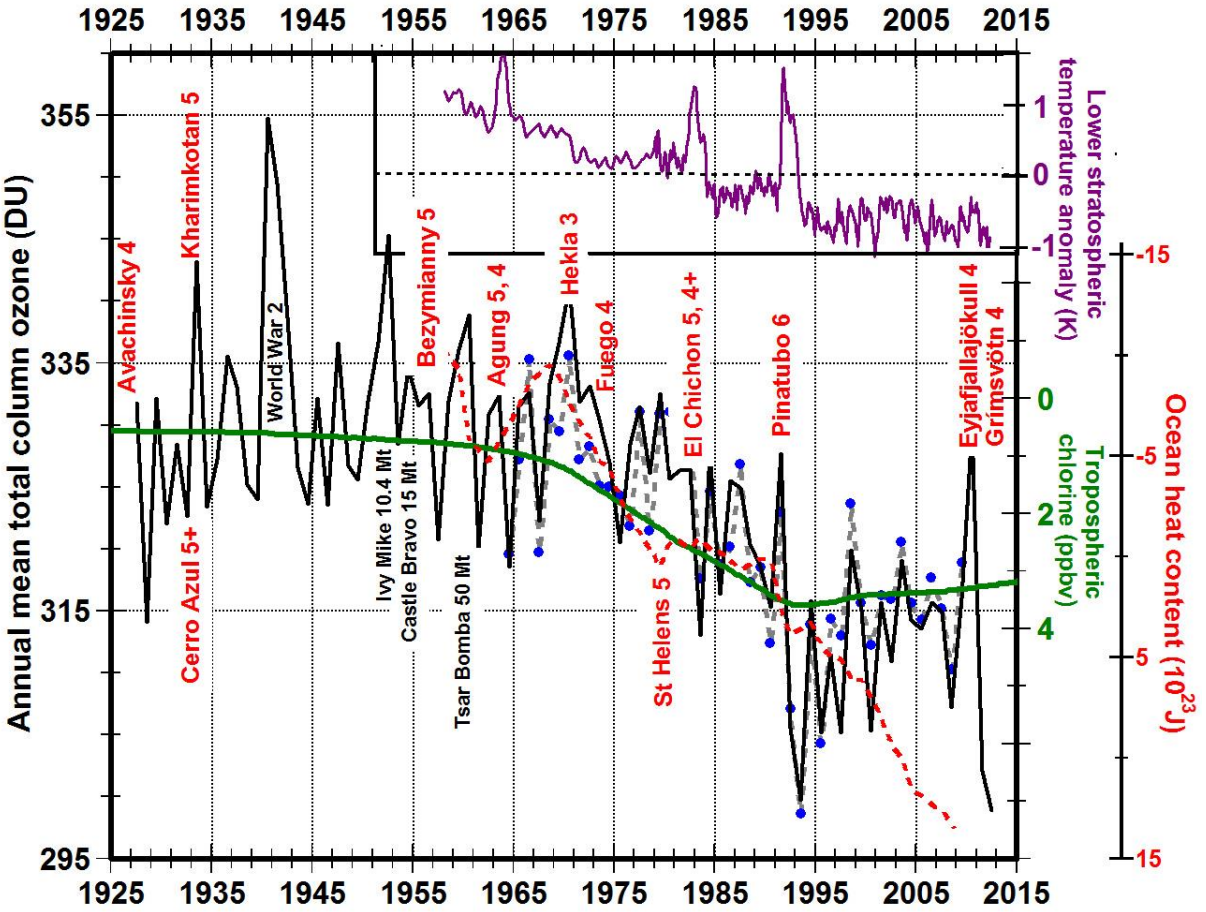

Figure 6. Annual mean total column ozone (black line) peaks during years with major volcanic eruptions and then drops precipitously by more than twice as much during the following year causing a cooling in the lower stratosphere (purple line). The ozone data were measured at Arosa, Switzerland (Maeder, 2013; WOUDC, 2013). The names of the erupting volcanoes and the Volcano Explosivity Index (VEI) for each large eruption are labelled in red (Global Volcanism Program, 2013). The green line shows annual mean tropospheric chlorine with the y-axis inverted (Solomon, 1999). The dashed red line with the y-axis inverted shows increase in ocean heat content (Levitus et al., 2012). The purple line shows lower stratospheric temperature anomaly based on radiosonde data before 1979 (Hadley Centre, 2013) and satellite data since (Remote Sensing Systems, 2012) smoothed with a seven-month centred running mean.

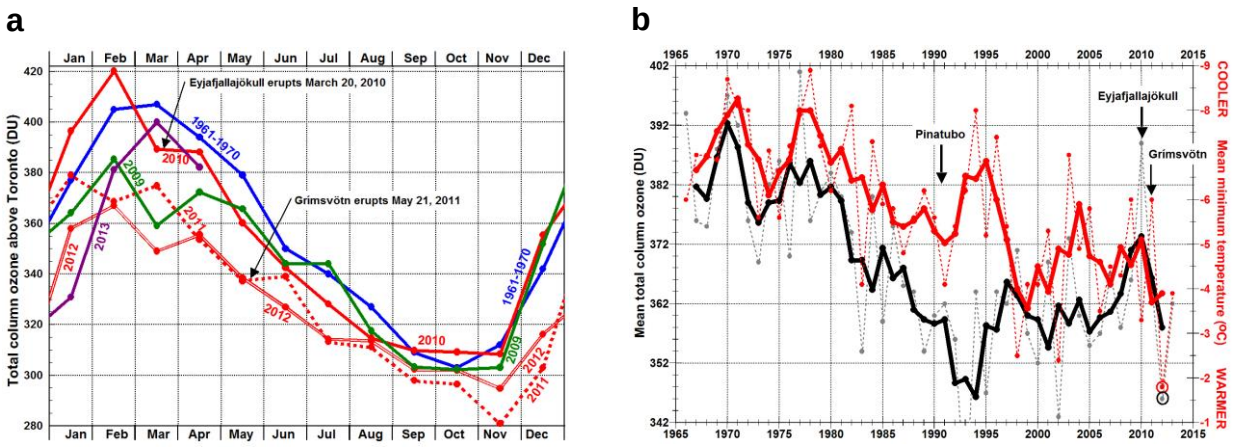

Figure 7. Ozone reached a minimum in 2012 when temperatures reached a maximum. a, Total column ozone above Toronto, Canada, in November, 2011, was 12% below the average for Novembers in 1961 through 1970 and has remained unusually low throughout 2012. b, When mean total column ozone measured during the months of December through April in Toronto Canada (black line) decreases, mean minimum temperature for the same months typically warms except following the eruption of Pinatubo (red lines, y-axis inverted). Ozone data measured at Environment Canada and the University of Toronto (WOUDC, 2013). Temperature data measured at Toronto International Airport (Environment Canada, 2013b). The dashed lines show annual means; the solid lines are smoothed using a 3-point centred running mean.

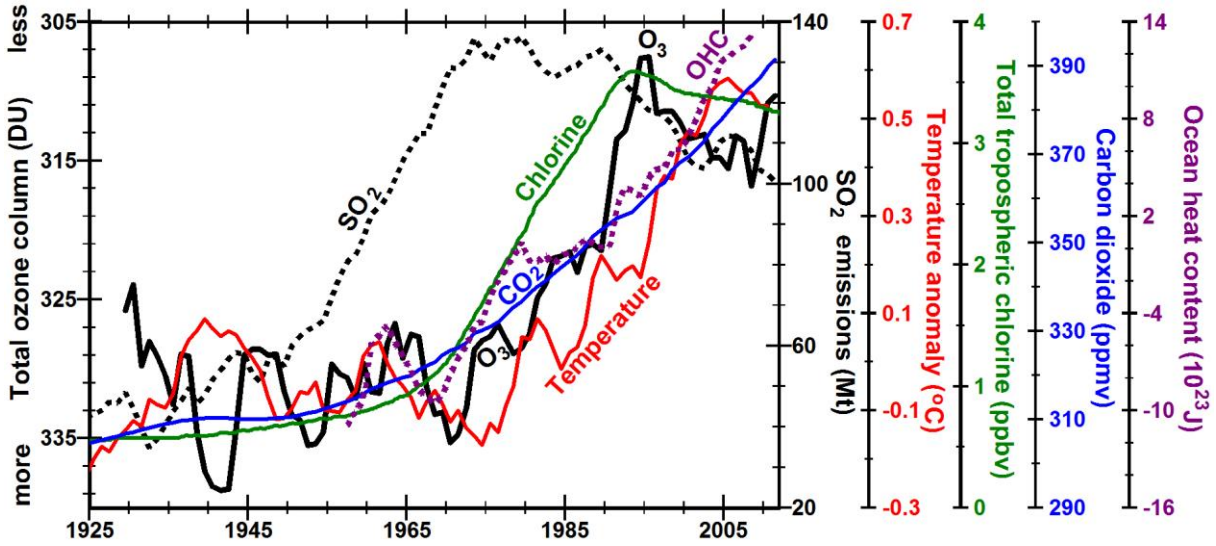

Figure 8. Increased SO_2 pollution (dotted black line) does not appear to contribute to substantial global warming (red line) until total column ozone decreased (black line, y-axis inverted), most likely due to increasing tropospheric chlorine (green line). Mean annual temperature anomaly in the Northern Hemisphere (red line) and ozone (black line) are smoothed with a centred 5 point running mean. OHC is ocean heat content (dotted purple line).

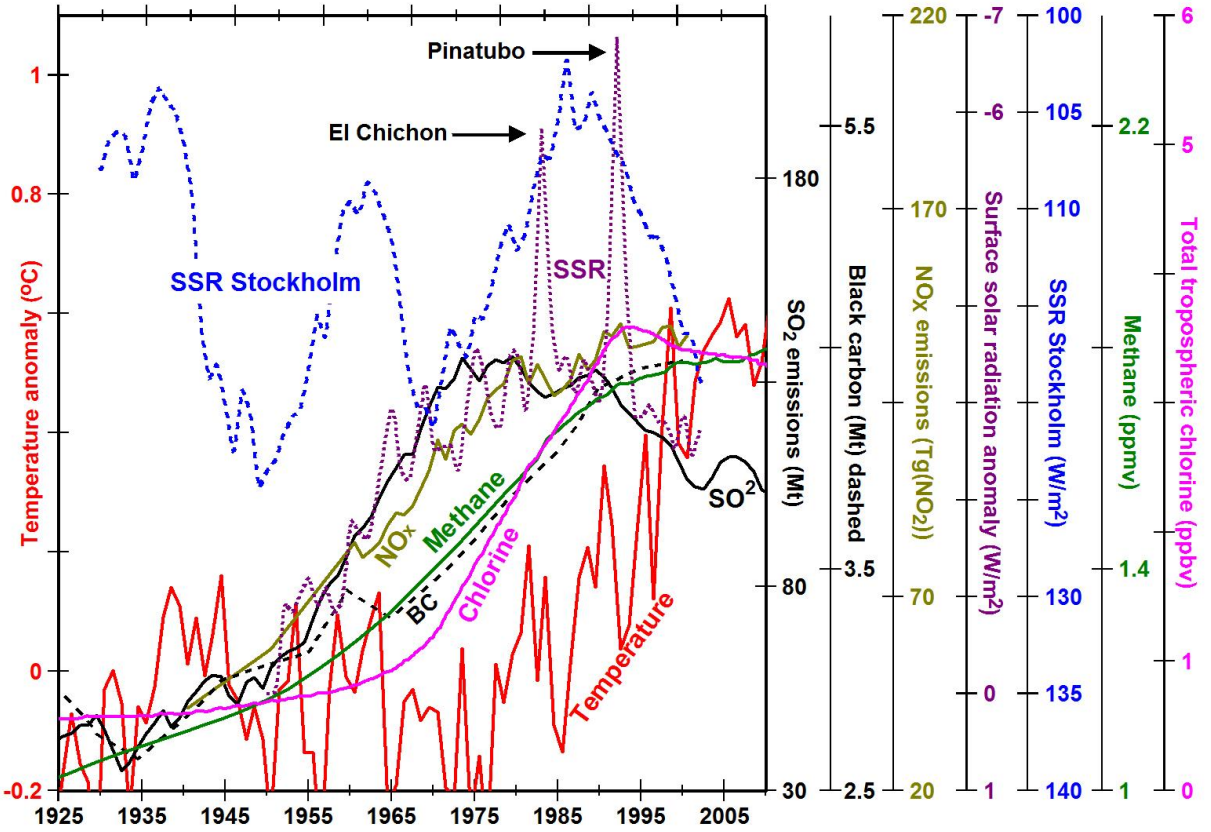

Figure 9. Surface solar radiation (SSR) observed at Stockholm (blue dashed line, y-axis inverted) does not show much similarity to SSR calculated theoretically (dotted purple line, y-axis inverted) from concentrations of pollutants such as SO_2, NO_X, and black carbon. NO_x data from RETRO (Schultz and Rast, 2008) interpolated before 1960 from US data (U. S. Environmental Protection Agency, 2000) are thought to be constant or slightly decreasing since 2000 (Cofala et al., 2009).

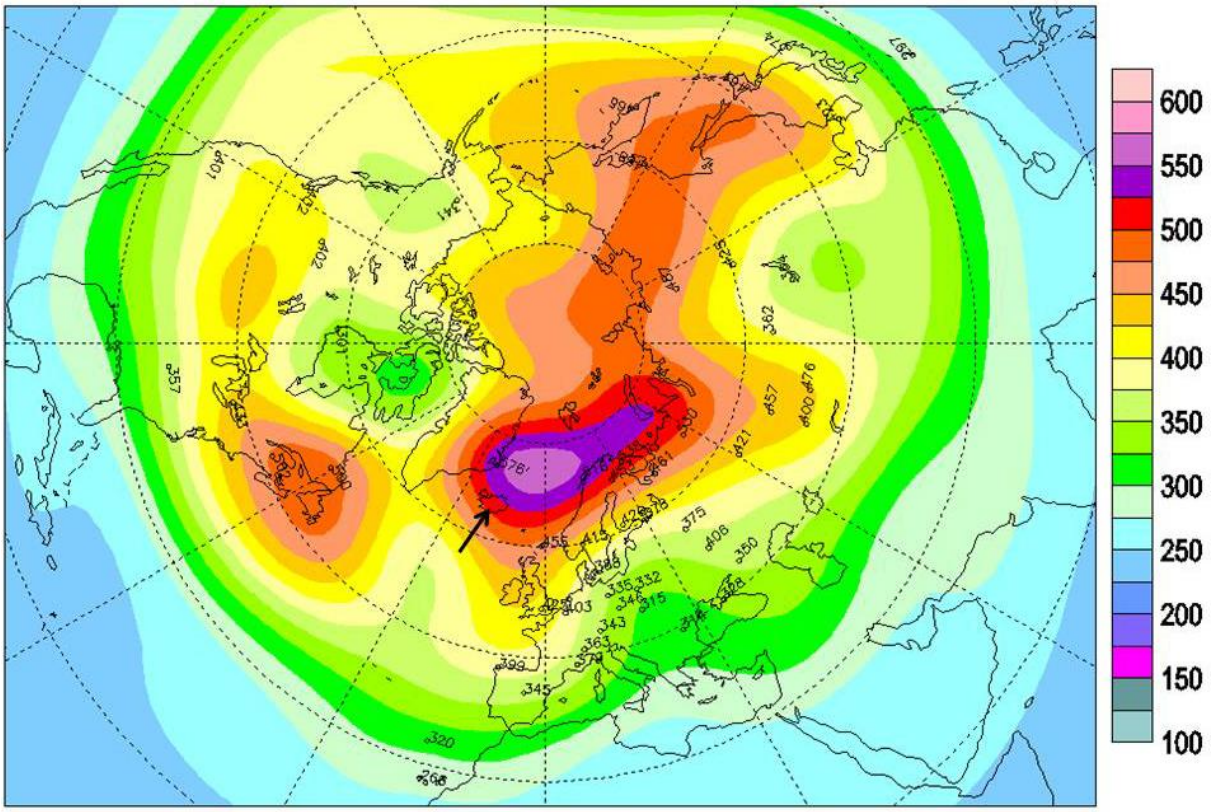

Figure B1. A total ozone anomaly >550 DU was observed northeast of Eyjafjallajökull volcano in South Iceland (black arrow) on 19 February 2010, based on the satellite borne Total Ozone Mapping Spectrometer (TOMS) integrated with data from ground stations.

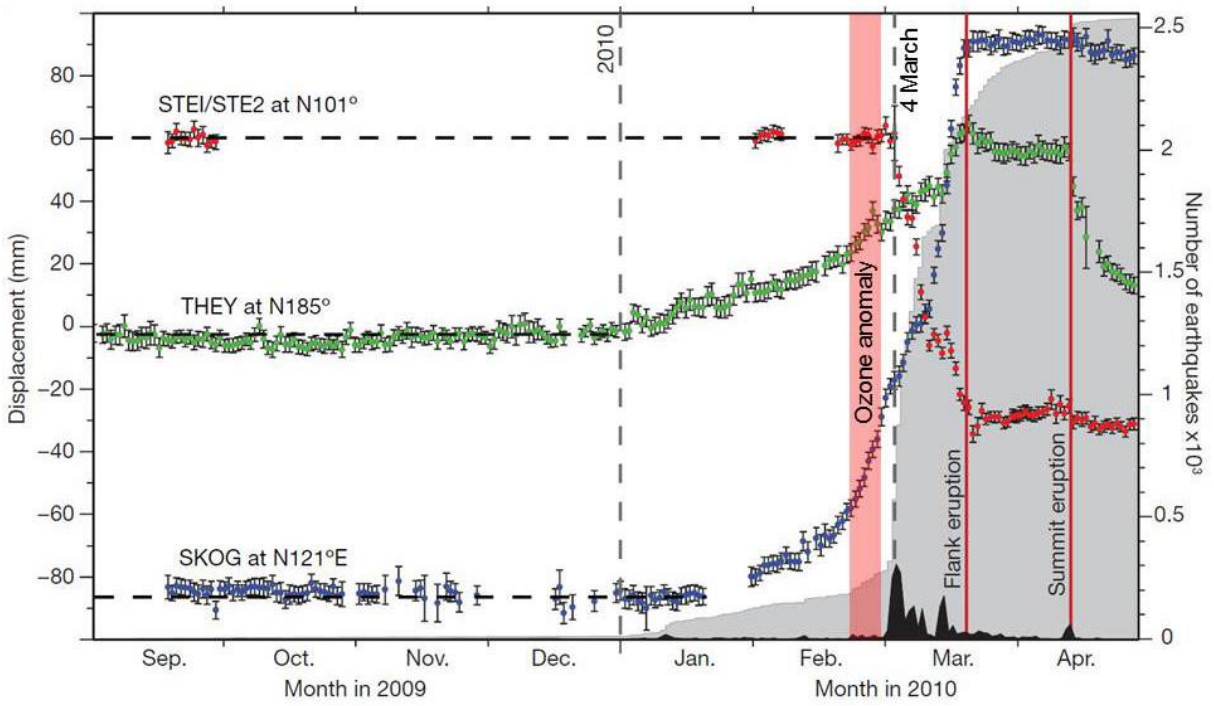

Figure B2. The ozone anomaly formed during the time shown by the red shaded area occurred just as surface displacement around Eyjafjallajökull (coloured dots with error bars) began to change quickly and the numbers of earthquakes began to increase. Black shows the daily number of earthquakes, grey the cumulative number. The first eruption of lava was on 20 March. Based on Figure 2 of Sigmundsson et al. (2010).

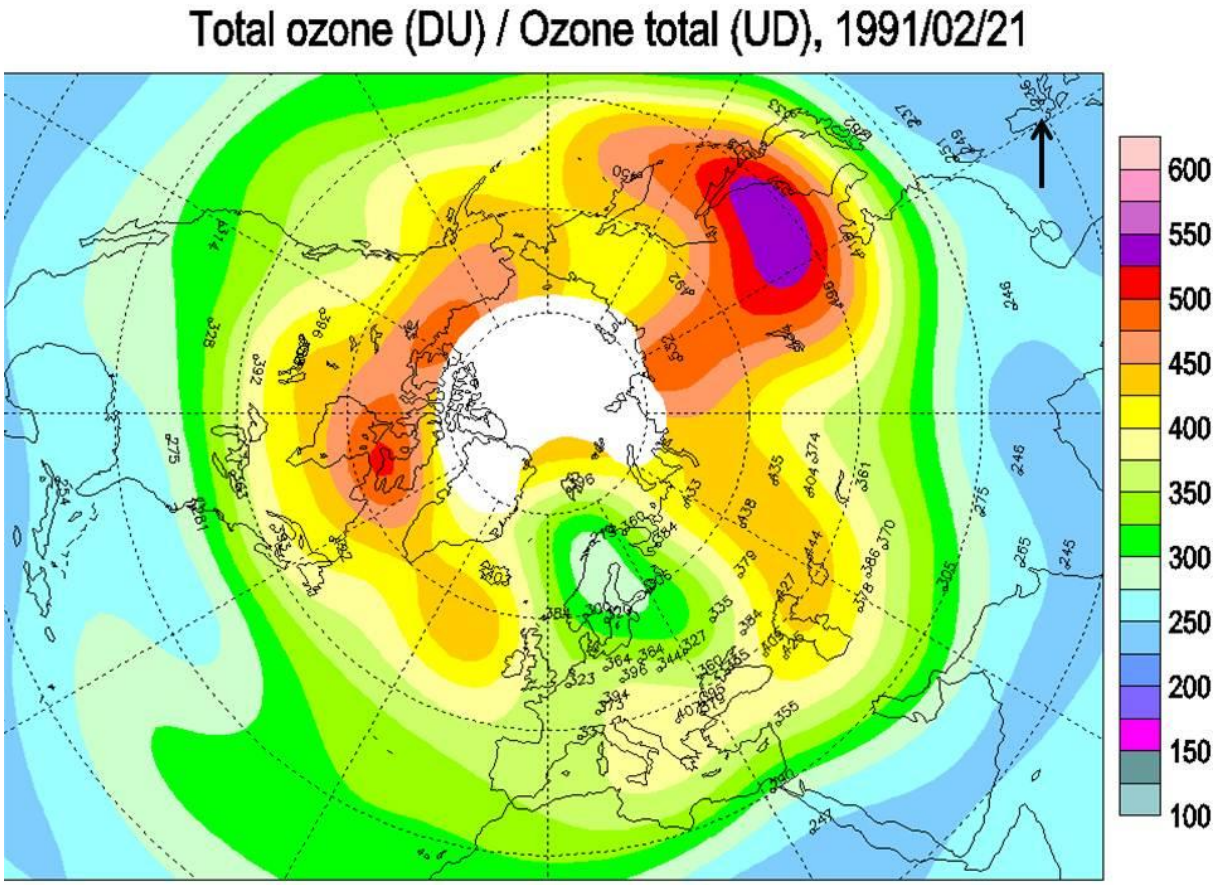

Figure B3. A total ozone anomaly >500 DU was observed from 20-22 February 1991 north of 44°N, where the Brewer-Dobson circulation would bring ozone emitted before the eruption of Pinatubo (black arrow at 15.1°N).